Cell Reports

Article

Aire suppresses CTLA-4 expression from the thymic stroma to control autoimmunity

Graphical abstract

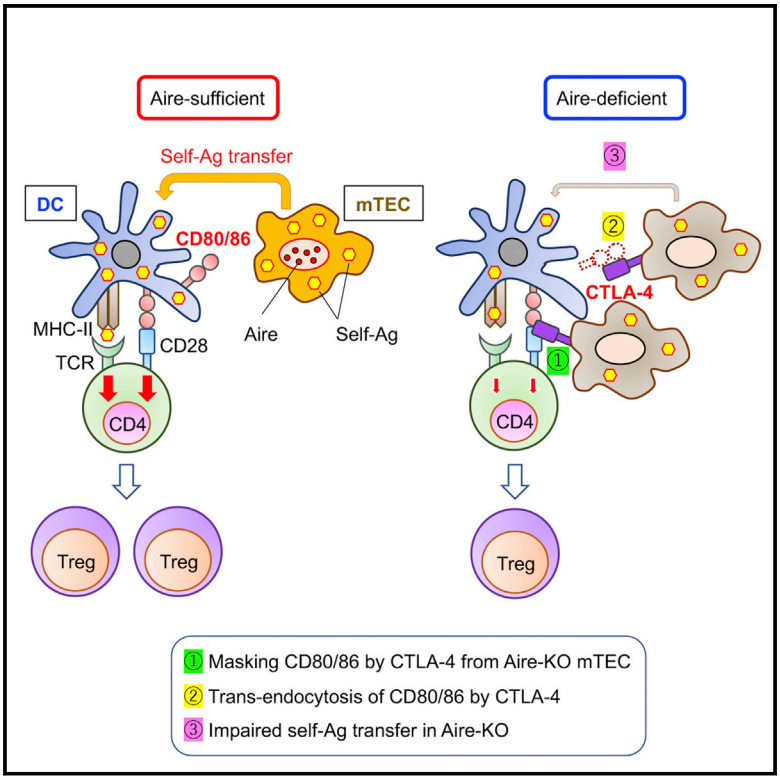

Highlights

- Impaired self-antigen expression from Aire-KO mTECs is responsible for autoimmunity
- Besides, Aire-KO mTECs abnormally expressed co-inhibitory receptor CTLA-4
- Ectopically expressed CTLA-4 from Aire-KO mTECs removed CD80/CD86 from thymic DCs
- Depleting CTLA-4 from Aire-KO mTECs rescued Treg production and autoimmunity

Authors

Junko Morimoto, Minoru Matsumoto, Ryuichiro Miyazawa, Hideyuki Yoshida, Koichi Tsuneyama, Mitsuru Matsumoto

Correspondence

mitsuru@tokushima-u.ac.jp

In brief

Searching for the mechanisms underlying Aire-dependent autoimmunity, Morimoto et al. show that CTLA-4 is ectopically expressed from Aire-deficient medullary thymic epithelial cells (mTECs), thereby removing the CD80/CD86 ligands from thymic DCs. Accordingly, impaired production of Tregs and organ-specific autoimmunity in Aire-deficient mice are rescued by depleting the CTLA-4 from mTECs.

Morimoto et al., 2022, Cell Reports *38*, 110384
February 15, 2022
https://doi.org/10.1016/j.celrep.2022.110384

CellPress

Cell Reports

CellPress
OPEN ACCESS

Article

Aire suppresses CTLA-4 expression from the thymic stroma to control autoimmunity

Junko Morimoto,[1] Minoru Matsumoto,[1,2] Ryuichiro Miyazawa,[1] Hideyuki Yoshida,[3] Koichi Tsuneyama,[2] and Mitsuru Matsumoto[1,4,*]

[1]Division of Molecular Immunology, Institute for Enzyme Research, Tokushima University, Tokushima 770-8503, Japan
[2]Department of Pathology and Laboratory Medicine, Tokushima University Graduate School of Biomedical Sciences, Tokushima 770-8503, Japan
[3]YCI Laboratory for Immunological Transcriptomics, RIKEN Center for Integrative Medical Science, Yokohama 230-0045, Japan
[4]Lead contact
*Correspondence: mitsuru@tokushima-u.ac.jp
https://doi.org/10.1016/j.celrep.2022.110384

SUMMARY

Impaired production of thymic regulatory T cells (Tregs) is implicated in the development of Aire-dependent autoimmunity. Because Tregs require agonistic T cell receptor stimuli by self-antigens to develop, reduced expression of self-antigens from medullary thymic epithelial cells (mTECs) has been considered to play a major role in the reduced Treg production in Aire deficiency. Here, we show that mTECs abnormally express co-inhibitory receptor CTLA-4 if Aire is non-functional. Upon binding with CD80/CD86 ligands expressed on thymic dendritic cells (DCs), the ectopically expressed CTLA-4 from Aire-deficient mTECs removes the CD80/CD86 ligands from the DCs. This attenuates the ability of DCs to provide co-stimulatory signals and to present self-antigens transferred from mTECs, both of which are required for Treg production. Accordingly, impaired production of Tregs and organ-specific autoimmunity in Aire-deficient mice are rescued by the depletion of CTLA-4 expression from mTECs. Our studies illuminate the significance of mTEC-DC interaction coordinated by Aire for the establishment of thymic tolerance.

INTRODUCTION

Since mutations in *Aire* were discovered to be responsible for a rather rare type of autoimmune disease in humans (autoimmune polyendocrine syndrome type 1: APS-1) showing Mendelian recessive inheritance, the mechanisms linking loss of autoimmune regulator (Aire) function with the development of autoimmunity have been a target of intensive research in immunology (Klein et al., 2014; Mathis and Benoist, 2009). This is because an understanding of the mechanisms underlying the autoimmune pathology caused by Aire deficiency would help to answer the fundamental question of how the immune system discriminates between self and non-self in the thymic microenvironment.

Expression of the whole-body transcriptome of tissue-restricted antigens (TRAs) from medullary thymic epithelial cells (mTECs) is critical for the establishment of immunological self-tolerance. Aire has been demonstrated to control the expression of many TRAs from mTECs, although the mechanisms underlying this phenomenon remain elusive, partly due to the low and promiscuous expression of TRAs (Anderson et al., 2002; Kyewski and Klein, 2006; Mathis and Benoist, 2009; Sansom et al., 2014; Tomofuji et al., 2020). In this regard, we have also noticed that Aire-dependent transcriptional control of TRAs in mTECs does not necessarily account for Aire-dependent autoimmunity in some cases (Kuroda et al., 2005). For example, we have identified pancreas-specific protein disulfide isomerase (PDIp) as an autoantigen recognized in Aire-deficient mice. However, the expression level of PDIp from Aire-deficient mTECs was not down-regulated (Niki et al., 2006). The results prompted us to search for other Aire-dependent autoimmune mechanisms besides Aire's control of TRA expression.

One pathological mechanism responsible for the development of autoimmunity in Aire-deficient patients is the defect in the regulatory T cells (Tregs) quantitatively and/or qualitatively (Hetemaki et al., 2016; Kekalainen et al., 2007; Laakso et al., 2010; Ryan et al., 2005). Because Tregs require agonistic T cell receptor (TCR) stimuli by self-antigens to develop (Sakaguchi et al., 2020) and Aire-expressing mTECs can directly present self-antigens for the production of Tregs (Aschenbrenner et al., 2007), reduced expression of TRAs from mTECs could account for the defect in the production of Tregs in Aire-deficient mice (Malchow et al., 2016; Yang et al., 2015). However, mTECs are not the only cell type that present self-antigens for the production of Tregs. Instead, dendritic cells (DCs), another antigen-presenting cell type in the thymus, also present self-antigens required for Treg production. In this case, thymic DCs not only present self-antigens produced by DCs and those of blood-borne origin, but they can also take up self-antigens produced by mTECs for the tolerance induction through a process called antigen transfer (Koble and Kyewski, 2009; Leventhal et al., 2016; Perry et al., 2018). However, the exact mechanisms for the antigen transfer that requires coordinated interaction between mTECs and DCs

have been characterized only incompletely. Because thymic DCs closely interact with Aire-expressing mTECs within the medulla (Nishikawa et al., 2010), it would be possible to speculate that thymic stroma-dependent altered function of DCs might also be responsible for the defect in the production of Tregs and ultimately for the development of organ-specific autoimmune disease caused by Aire deficiency.

In an effort to search for the molecules and/or pathways involved in Aire-dependent Treg production and autoimmunity, we discovered that co-inhibitory receptor cytotoxic T lymphocyte antigen-4 (CTLA-4) was ectopically expressed from Aire-deficient mTECs. Remarkably, abnormally expressed CTLA-4 from Aire-deficient mTECs altered the ability of thymic DCs to produce Tregs: ectopically expressed CTLA-4 from the mTECs captured the CTLA-4 ligands (i.e., CD80/CD86) expressed on DCs and reduced the co-stimulatory signals for Tregs to develop. Interestingly, this disturbance of the CD80/CD86-CD28 signals by CTLA-4 is an analogous strategy employed by Tregs to attenuate the antigen-presenting capacity of DCs in the periphery (Qureshi et al., 2011; Tekguc et al., 2021; Walker and Sansom, 2011; Wing et al., 2008). Furthermore, we found that reduced CD80/CD86-CD28 signals also impaired the self-antigen transfer from mTECs to thymic DCs that is required for the agonistic stimulation for Treg production. Thus, our findings demonstrated the significance of the mTEC-DC interaction coordinated by Aire and provided important implications for the spatial control of the expression of co-inhibitory molecule CTLA-4 by Aire for the maintenance of immune homeostasis.

RESULTS

Aire-deficient mTECs ectopically express co-inhibitory receptor CTLA-4

Transcriptomic analyses have revealed that the expression of many TRAs is down-regulated in mTECs from Aire-deficient mice (Aire-KO) (Anderson et al., 2002; Inglesfield et al., 2019; Sansom et al., 2014). Additionally, we anticipated that molecules expressed from mTECs in an Aire-dependent manner and responsible for autoimmunity might be detectable by conventional flow-cytometric analysis. In a search for such molecules, we found that CTLA-4 (CD152), a negative regulator of the T cell response whose blocking has achieved an effective cancer immunotherapy (Teft et al., 2006; Walker and Sansom, 2011), was expressed by 10–15% of mTECs expressing CD80 at high levels (mTEC^{high}) in Aire-KO, but not in wild-type mice (WT) (Figure 1A). It was noteworthy that detection of CTLA-4 with monoclonal antibodies (mAbs) incubated on ice required permeabilization of the cells for Aire-KO mTECs (Figure 1B, top), CD4^{+}Foxp3^{+} Tregs, and a small percentage of CD4^{+}Foxp3^{-} conventional T cells (Tconvs) with activated phenotypes from both WT and Aire-KO (Figure 1B, bottom). This was because CTLA-4 is constitutively internalized with a dynamic turnover (Linsley et al., 1996), making it difficult to detect its cell-surface expression. We analyzed in more detail which mTEC population(s) express CTLA-4 in Aire-KO. When we examined mice homozygous for the diphtheria toxin receptor (DTR)-GFP knockin allele in *Aire* loci (Aire$^{DTR\text{-}GFP}$ reporter mice) lacking functional Aire protein (Kawano et al., 2015), CTLA-4 was expressed predominantly from "Aire-less" GFP^{+} mature mTECs (Figure 1C), suggesting that ectopic expression of CTLA-4 from Aire-KO mTECs is primarily cell-autonomous.

Because there are three types of transcript for *Ctla-4* (Teft et al., 2006), we examined the transcript species of Aire-KO mTECs by real-time PCR. Aire-KO mTECs, but not WT mTECs, expressed transcripts for the full-length and ligand-independent forms but not the soluble form, in contrast to thymic Tregs from WT expressing all the three types (Figure 1D). CD4^{+}Foxp3^{-} Tconvs also expressed CTLA-4 transcripts of the full-length and ligand-independent forms at lower levels, consistent with the findings of flow-cytometric analysis (Figure 1B, bottom).

Altered heterogeneity of mTECs by the lack of Aire results in the aberrant expansion of mTECs expressing CTLA-4

We investigated the mechanisms underlying the ectopic expression of CTLA-4 from Aire-KO mTECs by performing single-cell (sc) RNA-seq analyses using FACS-sorted CD45^{-}EpCAM^{+} TECs from WT and Aire-KO mice (NCBI accession number GSE155331) (Nishijima et al., 2022). Fifteen clusters emerged, including Aire-expressing cluster 5 among CD80^{high} (mTEC^{high}) clusters (Nishijima et al., 2022). The proportion of mTEC^{high} clusters was changed by the loss of Aire: the proportion of clusters 1, 2, and 7 was increased, whereas that of clusters 4 and 5 was decreased in Aire-KO (Nishijima et al., 2022). Consistent with CTLA-4 expression from Aire-KO mTECs but not from WT mTECs by flow cytometry and real-time PCR, CTLA-4-expressing cells were evident only from Aire-KO (Figure 2A), and they were mainly in clusters 2, 3, 6, and 7 (Figure 2B). Gene ontology analysis of 649 up-regulated genes in these CTLA-4-expressing clusters compared with the other non-CTLA-4-expressing clusters (log2FC [fold change] > 0 and adjusted p value < 0.05 evaluated by Wilcoxon Rank-Sum test; Table S1) showed an association with "regulation of leukocyte-mediated immunity" and "regulation of T cell activation," consistent with the CTLA-4 function (Figure 2C). Thus, altered heterogeneity of mTECs by the lack of Aire resulted in the aberrant expansion of mTECs expressing CTLA-4.

Additionally, lower expression of miRNA-155, which inhibits CTLA-4 gene expression (Sonkoly et al., 2010) in Aire-KO mTEC^{high} compared with that in WT mTEC^{high}, may also contribute to the ectopic expression of CTLA-4 from Aire-KO mTECs (Figure 2D).

Ectopically expressed CTLA-4 from Aire-deficient mTECs captures CTLA-4 ligands

CTLA-4 expressed on Tregs is responsible for the suppression of the antigen-presentation capacity of DCs by masking and/or capturing the ligands (i.e, CD80 and CD86) from the cell surface by a process known as trans-endocytosis, thereby modulating the function of DCs (Qureshi et al., 2011; Tekguc et al., 2021; Walker and Sansom, 2011; Wing et al., 2008). To investigate whether CTLA-4 ectopically expressed by Aire-KO mTECs has such properties, we first examined the interaction between Aire-KO mTECs and recombinant CD80 protein (rCD80) in culture. Because rCD80 was produced as a fusion protein with human IgG$_1$ Fc, phycoerythrin (PE)-labeled anti-human IgG was

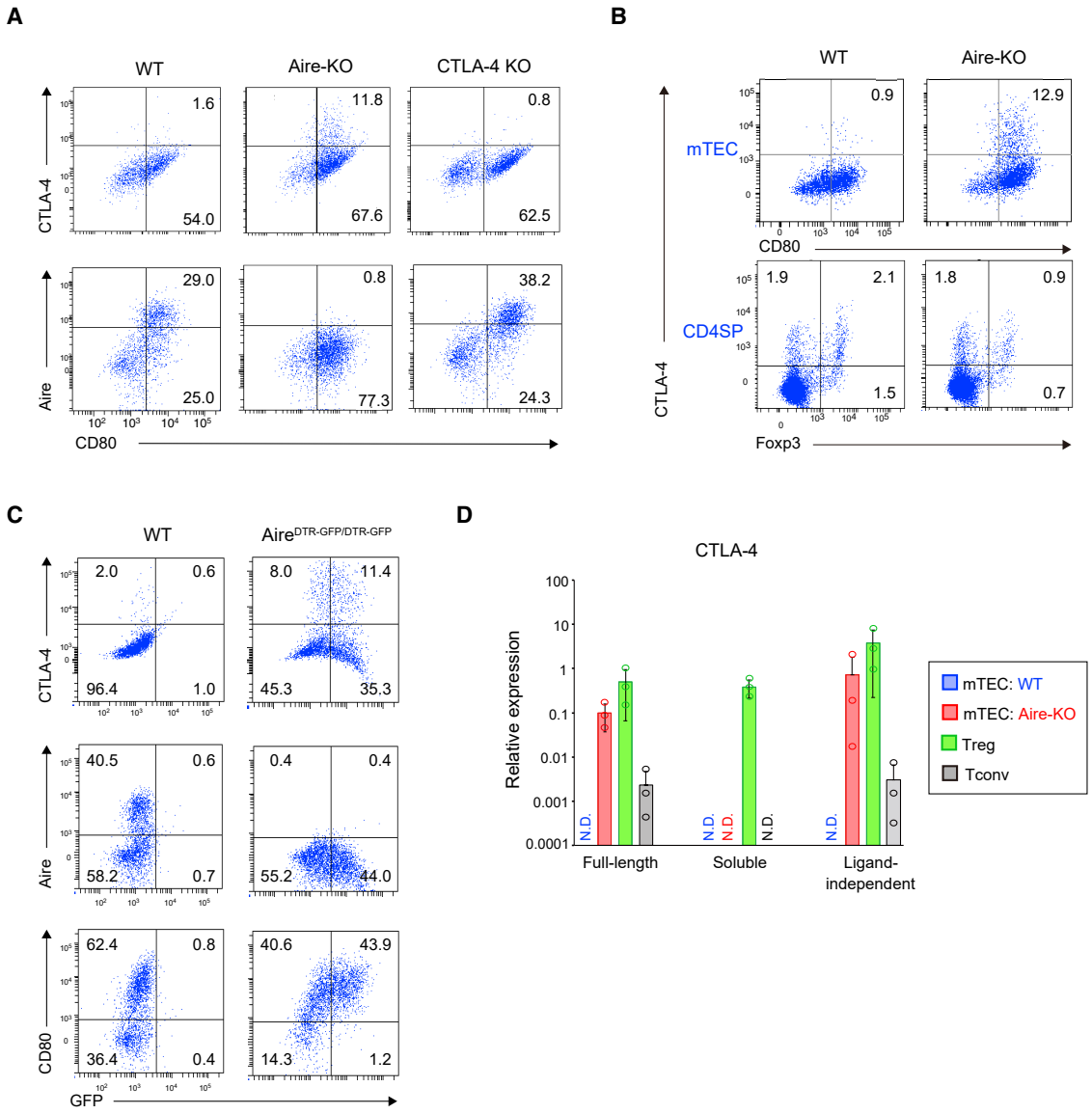

Figure 1. Aire-deficient mTECs ectopically express co-inhibitory receptor CTLA-4

(A) Flow-cytometric analysis of CTLA-4 expression from Aire-KO mTECs (gated for CD45$^-$EpCAM$^+$UEA-1$^+$ cells). CTLA-4-KO and Aire-KO mTECs served as negative controls for CTLA-4 (top) and Aire (bottom), respectively. One representative result from a total of three repeats is shown.

(B) Flow-cytometric analysis of CTLA-4 expression together with CD80 from mTECs (top) and with Foxp3 by CD4SP (bottom) in WT and Aire-KO. One representative result from a total of three repeats is shown.

(C) Flow-cytometric analysis of CTLA-4 expression from mTECs in mice homozygous for the DTR-GFP knockin allele in *Aire* loci (Aire$^{DTR-GFP}$-reporter strain) lacking functional Aire protein. Expressions of GFP together with CTLA-4 (top), Aire (middle), and CD80 (bottom) from mTECs are shown. Cells were gated for the CD45$^-$EpCAM$^+$UEA-1$^+$ population. One representative result from a total of four repeats is shown.

(D) Detection of the CTLA-4 transcripts for the full-length, soluble, and ligand-independent forms by using real-time PCR in mTECs (sorted for CD45$^-$EpCAM$^+$UEA-1$^+$ cells) from WT and Aire-KO. Tregs [CD25$^+$Foxp3 (GFP)$^+$ CD4SP] and Tconvs [CD25$^-$Foxp3 (GFP)$^-$ CD4SP] isolated from Foxp3/EGFP-knockin thymi were included for comparison. The level of *Gapdh* expression was used as an internal control. Data are triplicates of pooled mice ($n = 2$) and are one representative result of three independent experiments. Bars indicate means ± SD. N.D., not detected.

used for the detection. When pre-formed rCD80/PE-labeled anti-human IgG (PE-rCD80) was incubated with FACS-sorted non-permeabilized CD45$^-$EpCAM$^+$*Ulex europaeus* agglutinin 1 (UEA-1)$^+$ mTECs at 37°C, we observed the PE signals predominantly from mTEC^{high} in Aire-KO (Figure 3A, red line at the top), suggesting that CTLA-4 expressed from Aire-KO mTECs can capture the CD80 ligand. In contrast, neither mTEC^{high} nor mTEC^{low} in WT showed the PE signals (Figure 3A, blue line at the top). The uptake of PE-rCD80 by Aire-KO mTEC^{high} occurred not only when FACS-sorted mTECs were used but also when all thymic cells including thymocytes as well as mTECs were examined (i.e., bulk culture) (Figure 3A, red line at the bottom); similar

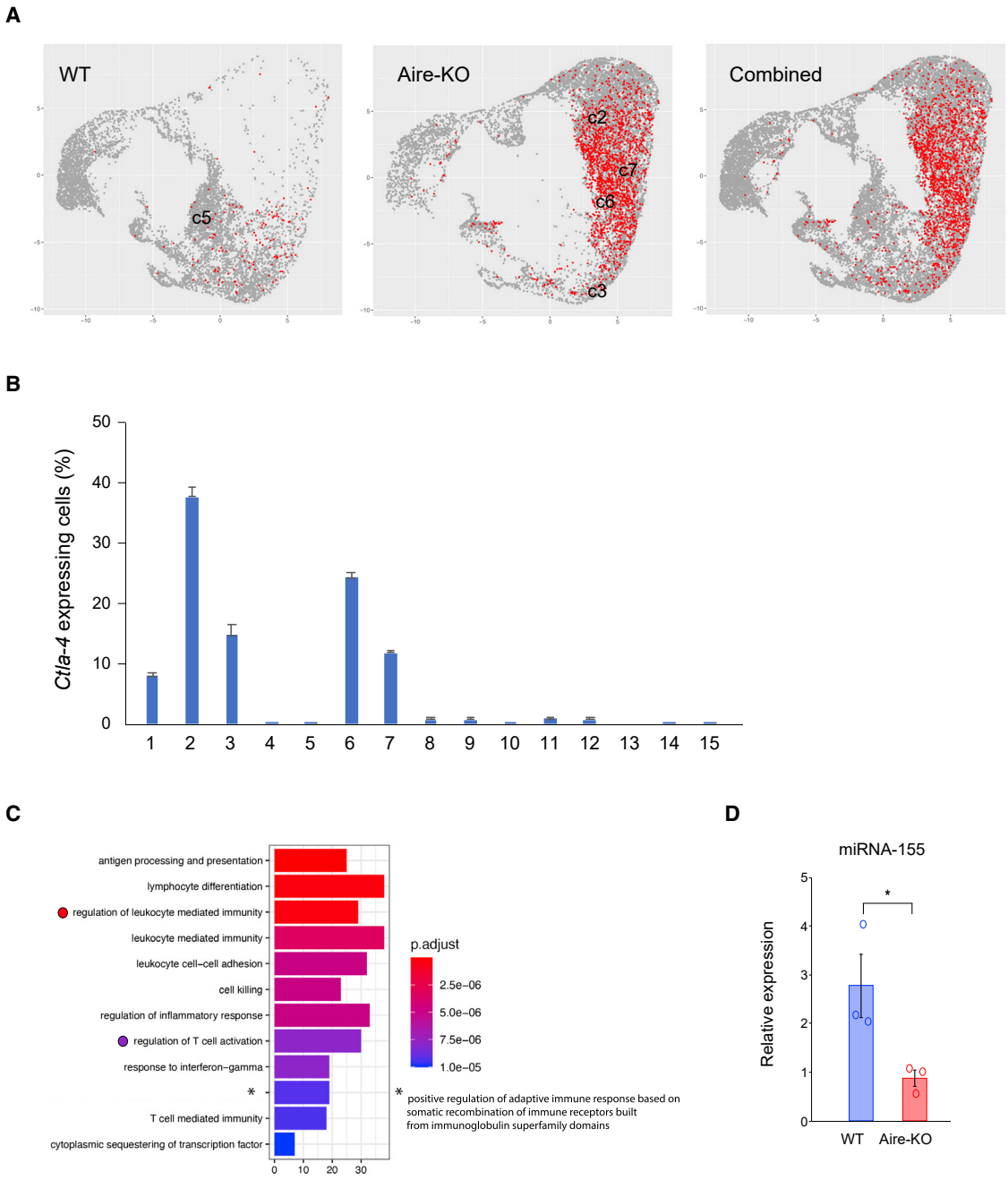

Figure 2. Altered heterogeneity of mTECs by the lack of Aire results in the aberrant expansion of mTECs expressing CTLA-4

(A) Expression of CTLA-4 for TEC clusters from WT (left) and Aire-KO (middle). Expression of CTLA-4 for TEC clusters from WT and Aire-KO both combined is also shown (right).

(B) Percentages of CTLA-4 expressing cells from each cluster among all the CTLA-4-expressing cells in Aire-KO. Cluster numbers are shown at the bottom. Bars indicate means ± SEM.

(C) Plot of the significantly enriched GO terms for the 649 up-regulated genes in clusters 2, 3, 6, and 7 from Aire-KO. Relevant terms are marked with filled circles colored with their adjusted p values. The gene list for the analysis is shown in Table S1.

(D) Detection of miRNA-155 expression from Aire-KO mTEC^{high} using real-time PCR. The level of snoRNA-202 expression was used as an internal control ($n = 3$ per group). Bars indicate means ± SEM. The significances were determined using unpaired two-tailed Student's t test. *$p < 0.05$.

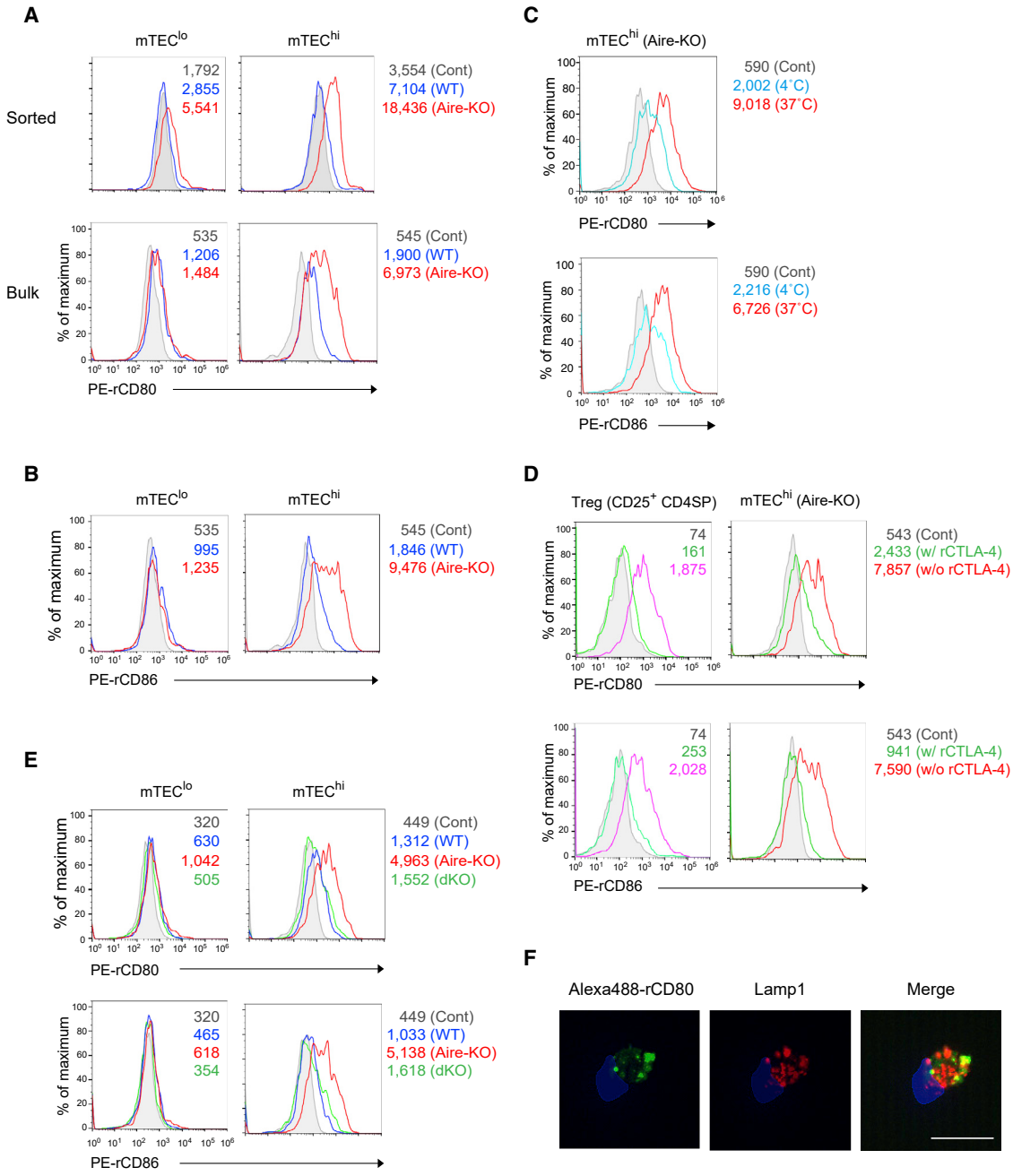

Figure 3. Ectopically expressed CTLA-4 from Aire-deficient mTECs captures CTLA-4 ligands

(A) Internalization of CTLA-4 complexed with pre-formed rCD80/PE-labeled anti-human IgG (PE-rCD80) by FACS-sorted (top) and bulk-cultured mTECs (bottom). Cells were incubated with PE-rCD80 at 37°C for 3 h, and PE-rCD80 signals in mTEC^{low} and mTEC^{high} after gating for CD45^{-}EpCAM^{+}UEA-1^{+} cells from WT (blue line) and Aire-KO (red line) were examined. PE-labeled anti-human IgG served as negative controls (gray shadow). Mean fluorescence intensities (MFIs) for each signal are included. One representative result from a total of three repeats is shown.

(B) Internalization of pre-formed rCD86/PE-labeled anti-human IgG (PE-rCD86) by mTECs from WT (blue line) and Aire-KO (red line) in the bulk culture as analyzed in (A). MFIs for each signal are included. One representative result from a total of three repeats is shown.

(C) Temperature-dependent uptake of PE-rCD80 (top) and PE-rCD86 (bottom) by Aire-KO mTECs. mTECs from Aire-KO in the bulk culture were incubated with PE-rCD80 or PE-rCD86 at 37°C (red line) or 4°C (light blue line) for 3 h and analyzed for mTEC^{high}. MFIs for each signal are included. One representative result from a total of three repeats is shown.

(D) Right: Internalization of PE-rCD80 (top) and PE-rCD86 (bottom) by Aire-KO mTEC^{high} in the presence (green line) or absence of rCTLA-4 (red line) as analyzed in (A). Left: Tregs (CD25^{+} CD4SP) from wild-type thymi served as a control with (green line) or without rCTLA-4 (magenta line). MFIs for each signal are included. One representative result from a total of three repeats is shown.

(legend continued on next page)

results were obtained when recombinant CD86 was used for the interaction (Figure 3B). Uptake of PE-rCD80 by CTLA-4 from Aire-KO mTECs was also observed when PE-rCD80 was injected directly into thymi from Aire-KO *ex vivo* (Figures S1A and S1B). These uptakes of PE-rCD80 and PE-rCD86 by Aire-KO mTECs occurred predominantly at 37°C but not at 4°C (Figure 3C), consistent with the temperature-dependent turnover of CTLA-4 (Linsley et al., 1996). Although PE-rCD80 and PE-rCD86 could bind with another receptor, CD28, mTECs did not express CD28, in contrast to CD4 and CD8 single-positive T cells (Figure S1C). Temperature-dependent internalization of CTLA-4 by Aire-KO mTECs was also detected when an anti-CTLA-4 mAb (clone UC10-4F10-11) was used for the incubation (Figure S1D), as observed for Tregs from WT (Figure S1E). Furthermore, uptake of PE-rCD80 and PE-rCD86 by CTLA-4 from Aire-KO mTECs was inhibited by the presence of recombinant CTLA-4 (rCTLA-4) during the incubation, similarly to $CD25^{+}CD4^{+}$ Tregs (Figure 3D, green line), further confirming the specificity of the interaction between CTLA-4 expressed from Aire-KO mTECs and its ligands. Most convincingly, we did not detect internalization of PE-rCD80 (Figure 3E, green line at the top) and PE-rCD86 (Figure 3E, green line at the bottom) by $mTEC^{high}$ isolated from neonatal mice lacking both Aire and CTLA-4 (dKO).

Immunocytochemical analysis showed that signals of Alexa 488-labeled rCD80 internalized by Aire-KO mTECs partially overlapped with the endosomal pathway containing Lamp1 (CD107a; Figure 3F), consistent with the intracellular trafficking of CTLA-4 (Valk et al., 2008). Taken together, these results suggested that ectopically expressed CTLA-4 from Aire-KO mTECs could capture the CD80/CD86 ligands as Tregs.

Ectopically expressed CTLA-4 from Aire-deficient mTECs captures CTLA-4 ligands expressed on thymic DCs

To investigate whether ectopically expressed CTLA-4 from Aire-KO mTECs could interact with authentic CD80/CD86 ligands expressed on bone-marrow-derived antigen-presenting cells (BM-APCs) in the thymus *per se*, we first analyzed the composition and function of BM-APCs in the thymus from WT in detail. $CD45^{+}$ cells harvested from collagenase/disperse-digested thymi were examined for their expression of CD11b and CD11c, and five major populations emerged (Figure 4A): $CD11b^{-}CD11c^{int}$ cells (P1), $CD11b^{-}CD11c^{+}$ cells (P2), $CD11b^{int}CD11c^{+}$ cells (P3), $CD11b^{+}CD11c^{int}$ cells (P4), and $CD11b^{+}CD11c^{-}$ cells (P5). By staining with several markers, P4 and P5 were identified as eosinophils and granulocytes because of their high expression of Siglec-F and Gr-1, respectively (Figure 4B). CD11c-positive P2 and P3 cells expressed high levels of major histocompatibility complex II (MHC-II) and CD80/CD86, indicating that they are DCs. Because P2 and P3 expressed high levels of CD103 and surface receptor signal-regulatory protein α (Sirpα), respectively, they corresponded to cDC1 ($CD8\alpha^{+}$ DC) and cDC2 ($Sirp\alpha^{+}$ DC) (Murphy et al., 2016). Levels of CD80/CD86 expression from P1 cells were slightly lower than those from P2 and P3 cells, suggesting that this population may be DCs in a transitional state before full maturation.

If ectopically expressed CTLA-4 from Aire-KO mTECs could capture the CD80/CD86 ligands *in vivo*, as suggested by the *in vitro* data demonstrated above, the expression levels of CD80/CD86 on thymic BM-APCs would become lower. Because CD80 but not CD86 has been reported to form the heterodimeric complex with PD-L1 *in cis* (Sugiura et al., 2019) and this PD-L1/CD80 heterodimeric complex protects CD80 from CTLA-4-mediated trans-endocytosis (Zhao et al., 2019), we focused on the CD86 expression. All the thymic BM-APCs showed significantly reduced levels of CD86 using anti-CD86 mAb (Figure 4C, left); the same results were obtained using rCTLA-4 as a probe except for P1 cells (Figure 4C, right). Of note, reduced expression of CTLA-4 ligands was observed only from thymic BM-APCs and not from splenic BM-APCs ($CD11c^{high}CD11b^{high}$ DCs, $CD11c^{high}CD11b^{low}$ DCs, and B cells) in Aire-KO (Figure S2A), suggesting that reduced expression of CTLA-4 ligands from BM-APCs is a thymus-specific event, as expected.

To further confirm that ectopically expressed CTLA-4 from Aire-KO mTECs is capturing CTLA-4 ligands *in vivo*, we injected blocking mAb against CTLA-4 (clone UC10-4F10-11) (Marangoni et al., 2021) and measured CD86 expression from BM-APCs. Injection of the CTLA-4-blocking mAb significantly increased the CD86 expression from all the thymic BM-APCs in Aire-KO to the same level of that from WT injected with the same mAb or with the isotype control (Figure 4D, left); note that injection of the CTLA-4 blocking mAb into WT showed no effect. The same treatment showed no effect on the CD86 expression from splenic BM-APCs (Figure 4D, right), which is consistent with the unaffected expression of CTLA-4 ligands from splenic BM-APCs as described above (Figure S2A). Thus, ectopically expressed CTLA-4 from Aire-KO mTECs could capture the co-stimulatory ligands *in vivo*, and this may alter the function of thymic DCs. The frequencies of the BM-APCs (i.e., P1 to P3) and eosinophils (P4) in the thymus were comparable between WT and Aire-KO (Figure S2B).

We have previously demonstrated the role of antigen presentation by thymic BM-APCs in the production of clonotypic Tregs (OT-II) by using MHC class II-deficient BM-APCs (Mouri et al., 2017). Here, we focused on the importance of thymic DCs for the production of Tregs in a polyclonal setting by generating BM chimeras transferred with BM cells from CD11c-DTR/GFP-transgenic mice (CD11c-DTR/GFP-Tg) (Jung et al., 2002). Upon continuous DT injection, these chimeras showed reduced production of Tregs (Figure S2C) following the reduction of thymic DCs (Figure S2D) without altering the production of $Aire^{+}$ mTECs (Figure S2E). Because this genetic ablation of all

(E) Internalization of PE-rCD80 (top) and PE-rCD86 (bottom) by mTECs taken from neonatal mice lacking both Aire and CTLA-4 (green line) as analyzed in (A). Signals obtained from wild-type mTECs incubated with PE-rCD80 (top, blue line) or PE-rCD86 (bottom, blue line) and Aire-KO mTECs incubated with PE-rCD80 (top, red line) or PE-rCD86 (bottom, red line) are shown for comparison. MFIs for each signal are included. One representative result from a total of three repeats is shown.

(F) Immunocytochemical analysis of signals for internalized CTLA-4 complexed with rCD80 in Aire-KO mTECs. Signals of Alexa 488-rCD80 (green), Lamp1 (red), and DAPI (blue) are shown. Scale bar: 10 μm. One representative datum from a total of three repeats is shown. See also Figure S1.

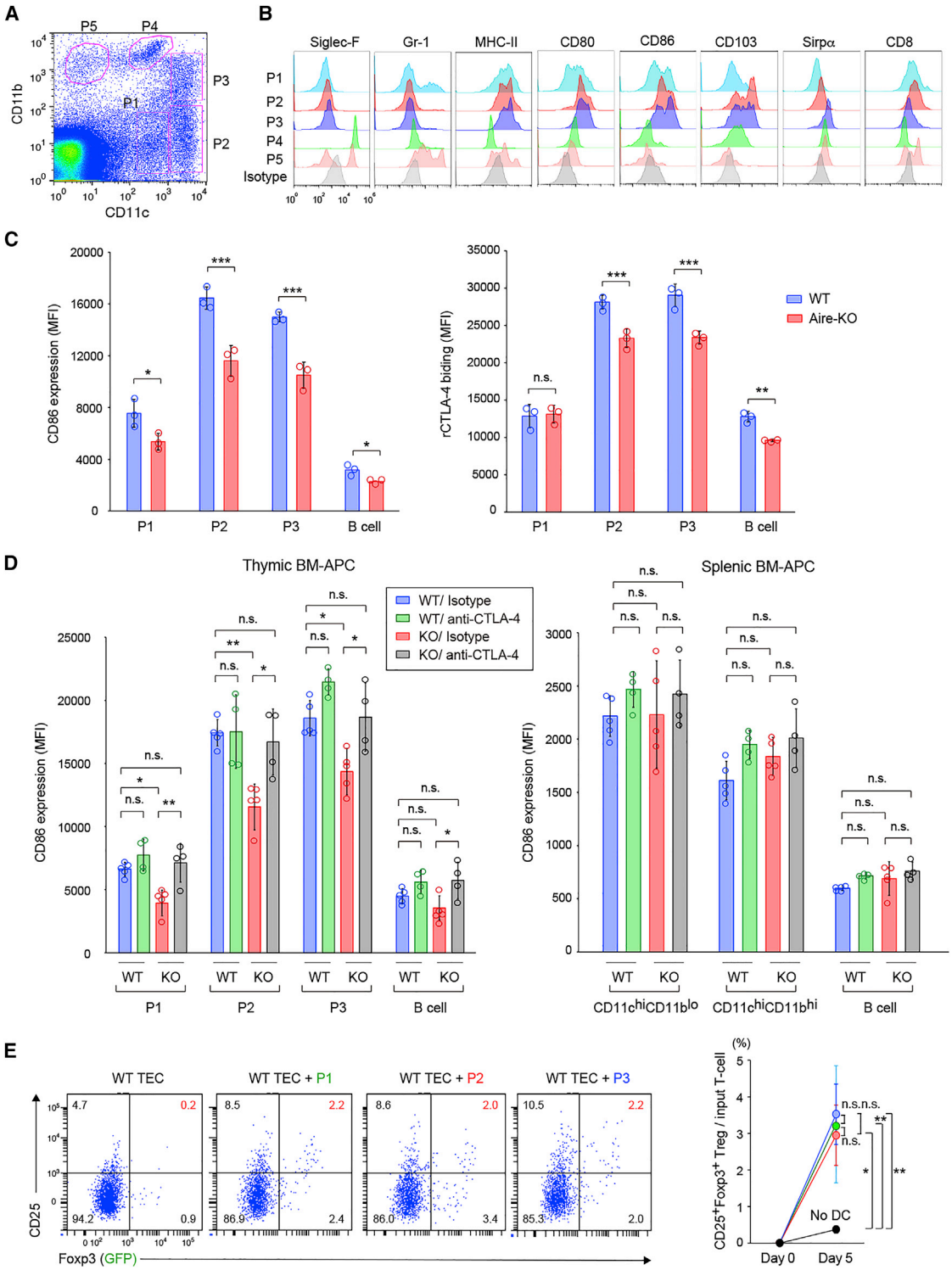

Figure 4. Ectopically expressed CTLA-4 from Aire-deficient mTECs captures CTLA-4 ligands expressed on thymic DCs

(A) Flow-cytometric analysis of BM-APCs in the thymus from WT defined by expression of CD11c and CD11b. Cells were gated for $CD45^+$ cells. The P1 to P5 populations are surrounded by magenta lines. One representative result from a total of more than three repeats is shown.

(B) Expressions of cell-surface markers by P1 to P5 cells shown in (A). Staining with isotype controls is shown at the bottom. One representative datum from a total of more than three repeats is shown.

(legend continued on next page)

the CD11c$^+$ DCs, however, did not address the Treg production ability of each DC population (i.e., P1 to P3), we next performed re-aggregated thymic organ culture (RTOC) (Figure S2F). When we generated RTOCs using embryonic TECs from WT without including BM-APCs, CD25$^+$Foxp3$^+$ mature Tregs were not produced from Treg precursors isolated from Foxp3-EGFP knockin mice (Figure 4E). In contrast, the addition of any P1 to P3 cells into the RTOCs induced significant numbers of CD25$^+$Foxp3$^+$ mature Tregs (Figure 4E), suggesting that all the P1 to P3 thymic DCs can contribute to the production of Tregs. Knowing this, we next examined whether ectopically expressed CTLA-4 from Aire-deficient mTECs might have any impact on the production of Tregs because expression of CTLA-4 ligands from thymic BM-APCs was reduced in Aire-KO (Figure 4C).

Aire deficiency impairs the production of Tregs through the aberrant expression of CTLA-4 from mTECs

Because Aire has been reported to control the recirculation of Tregs back to the thymus from the periphery (Cowan et al., 2018), we examined the production of CD25$^+$Foxp3$^+$ mature Tregs together with two distinct types of Treg precursors (i.e., CD25$^+$Foxp3$^-$ and CD25$^-$Foxp3$^+$ cells) (Owen et al., 2019; Tai et al., 2013) after excluding the CD44^{high} recirculating Tregs (Smigiel et al., 2014). Aire-KO showed a reduction of CD25$^+$Foxp3$^+$ mature Tregs together with CD25$^-$Foxp3$^+$ but not with CD25$^+$Foxp3$^-$ Treg precursors in the thymus (Figure 5A). We then confirmed that reduced production of Tregs in Aire-KO was mediated by the thymic stroma, using the RTOC system in which recirculation events are irrelevant (Figure S2F). Embryonic TECs from Aire-KO showed reduced production of Tregs compared with those from WT when P2 cells from WT were used for BM-APCs in the RTOCs (Figure S3A). Conversely, when RTOCs were generated using WT TECs together with P2 cells from Aire-KO, Tregs were produced normally (Figure S3B). Taking the results from Figure 4E (i.e., all the P1 to P3 thymic DCs could contribute to the production of Tregs) together, the data from the RTOCs suggested that production of Tregs was dependent on thymic DCs together with thymic stroma expressing Aire.

Because agonistic TCR signals by self-antigens are critical for the production of Tregs (Li and Rudensky, 2016; Sakaguchi et al., 2020) and Aire$^+$ mTECs can directly present self-antigens (Aschenbrenner et al., 2007), reduced expression of TRAs in Aire-KO mTECs might account for the reduced production of Tregs (Malchow et al., 2016; Yang et al., 2015). However, given that expression levels of CTLA-4 ligands on thymic DCs were reduced in Aire-KO by the ectopic CTLA-4 expression from mTECs (Figure 4C) and that co-stimulatory signals through CD28 on Treg-committed cells are required for full differentiation into Tregs (Salomon et al., 2000; Tai et al., 2005), aberrant expression of CTLA-4 from mTECs could also be responsible for the reduced Tregs in Aire-KO. We examined this possibility by the intraperitoneal (i.p.) injection of CTLA-4 Ig into WT to capture the CD80/CD86 ligands on thymic DCs and inhibit the CD28 signals in T cells, mimicking the aberrant expression of CTLA-4 from Aire-KO mTECs. WT mice inoculated with CTLA-4 Ig showed reduced production of CD25$^+$Foxp3$^+$ mature Tregs and CD25$^-$Foxp3$^+$ Treg precursors, but not CD25$^+$Foxp3$^-$ Treg precursors, in the thymus (Figure 5B), the same pattern as what we have seen in Aire-KO (Figure 5A). The results suggested that ectopically expressed CTLA-4 from Aire-KO mTECs attenuated CD80/CD86-CD28 signals required for the Treg production through modulating the function of thymic DCs.

We then confirmed the contribution of ectopically expressed CTLA-4 from Aire-KO mTECs to the impaired production of Tregs by generating mice deficient for both Aire and CTLA-4 (i.e., Aire/CTLA-4-dKO) to prepare Aire-KO thymic stroma that could not express CTLA-4 (Figure S3C). We first found that the production of mature CD25$^+$Foxp3$^+$ Tregs together with CD25$^+$Foxp3$^-$ and CD25$^-$Foxp3$^+$ precursors in CTLA-4-KO was comparable to that from WT when the mice were analyzed 9 days after birth before the onset of autoimmune disease. Remarkably, reduced production of mature CD25$^+$Foxp3$^+$ Tregs and CD25$^-$Foxp3$^+$ precursors in Aire-KO were rescued by the simultaneous depletion of CTLA-4 (Figure 5C). Interestingly, this took place with the remaining reduced expression of prototypic Aire-dependent TRAs such as *Sap* and *Ins2* from Aire/CTLA-4-dKO mTECs (Figure S3D). The results suggested that ectopically expressed CTLA-4 from Aire-KO mTECs contributed to the impaired production of Tregs in Aire-KO. The results also suggested the importance of cross talk between DCs and stromal cells expressing Aire within the medulla. This view was supported by the close contact between thymic DCs and "Aire-less" GFP$^+$ mTECs expressing CTLA-4 in homozygous Aire/GFP knock-in mice (Aire$^{GFP/GFP}$-reporter strain) (Yano et al., 2008) with immunohistochemical analysis (Figure S3E).

Blocking the CD80/CD86-CD28 signals attenuates the self-antigen transfer

Provision of agonistic TCR signals by antigen-presenting cells in the thymus (e.g., mTECs and DCs) is critical for the production of Tregs besides the co-stimulatory signals discussed above (Li

(C) Expression of CTLA-4 ligands on thymic BM-APCs. Anti-CD86 mAb (left) and rCTLA-4 (right) were used for detection by flow cytometry. Expression levels were determined by the MFIs. WT (n = 3) cells are shown in blue and Aire-KO (n = 3) cells are shown in red. Bars indicate means ± SD. One representative datum from a total of three repeats is shown.

(D) Rescue of the reduced CD86 expression from thymic BM-APCs in Aire-KO by injecting blocking mAb against CTLA-4. Mice were injected i.v. with 1.5 mg of anti-CTLA-4 mAb or isotype control. Forty-eight h later, thymic BM-APCs (left) and splenic BM-APCs (right) were isolated, and expression levels of CD86 were determined by the MFIs with flow cytometry. WT cells injected with isotype control (n = 5, blue), WT cells injected with anti-CTLA-4 mAb (n = 4, green), Aire-KO cells injected with isotype control (n = 5, red), and Aire-KO cells injected with anti-CTLA-4 mAb (n = 4, black) are shown. Bars indicate means ± SD.

(E) Production of mature CD25$^+$Foxp3$^+$ Tregs with RTOCs (Figure S2F). P1 (green), P2 (red), and P3 cells (blue) were used as BM-APCs with embryonic TECs, both isolated from WT. RTOCs without BM-APCs are marked with black circles (right). Percentages of CD25$^+$Foxp3$^+$ Tregs generated among input T cells were plotted for each RTOC. Collated data from four independent experiments are presented (right), and one representative result is shown on the left. Bars indicate means ± SD. Significances were determined using unpaired two-tailed Student's t test (C) or one-way ANOVA coupled with Tukey's multiple comparison test (D and E). *p < 0.05, **p < 0.01, ***p < 0.005; n.s., not significant. See also Figure S2.

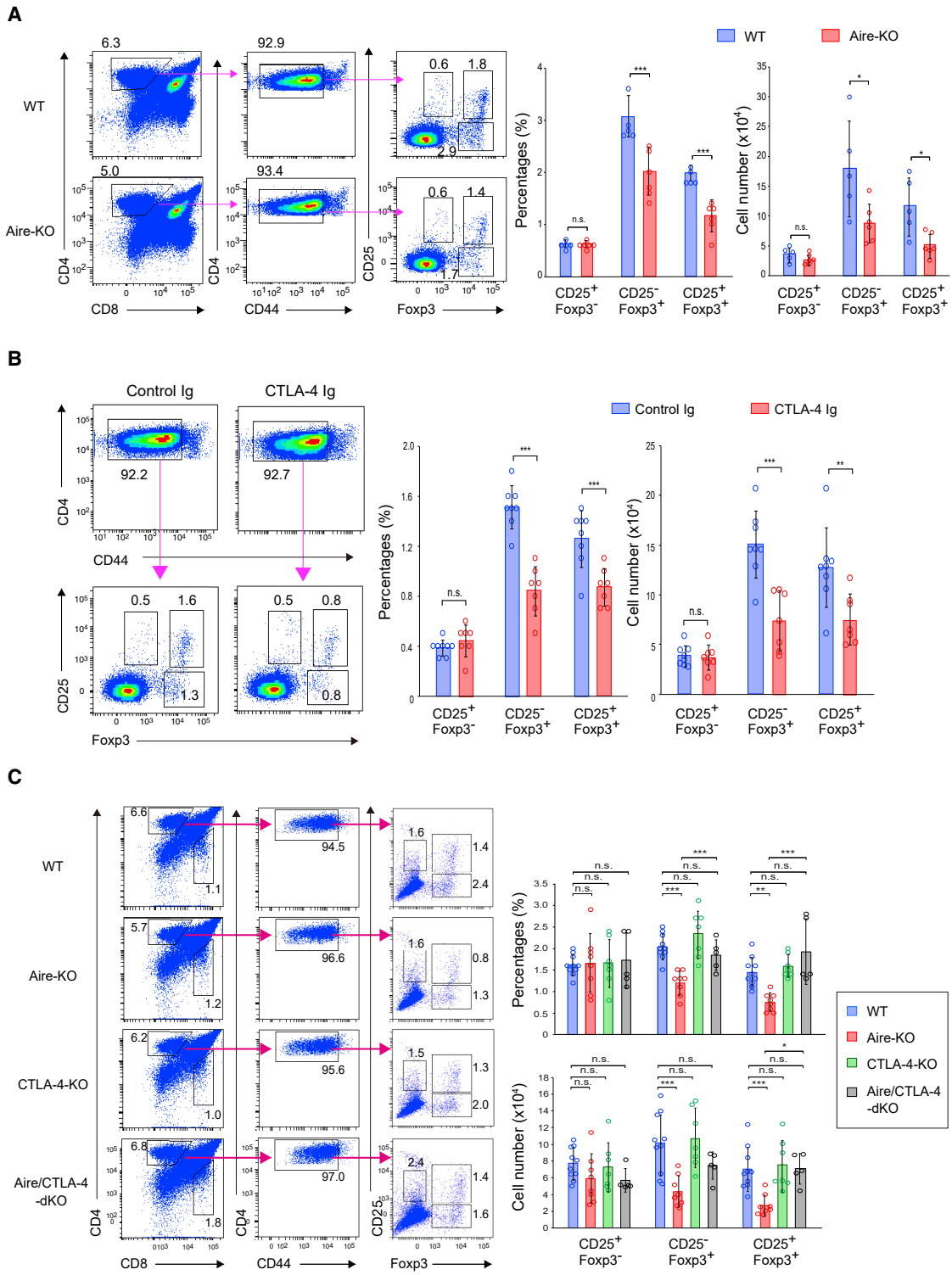

Figure 5. Aire deficiency impairs the production of Tregs through the aberrant expression of CTLA-4 from mTECs

(A) Percentages and numbers of thymic Tregs and Treg precursors in Aire-KO. Data were pooled from two independent experiments (n = 5 for WT and n = 6 for Aire-KO). Representative profiles of flow cytometry are shown on the left. Bars indicate means ± SD.

(B) Percentages and numbers of thymic Tregs and Treg precursors in wild-type B6 mice after injection of recombinant CTLA-4/human IgG Fc fusion protein (CTLA-4 Ig). Human IgG (Control Ig) was injected as a control. Data were pooled from two independent experiments (n = 8 for control Ig and n = 7 for CTLA-4 Ig). Representative profiles of flow cytometry are shown on the left. Bars indicate means ± SD.

(legend continued on next page)

and Rudensky, 2016; Sakaguchi et al., 2020). One interesting feature of thymic DCs is that they acquire self-antigens from mTECs through a unique process known as antigen transfer (Koble and Kyewski, 2009; Leventhal et al., 2016; Perry et al., 2018). However, the mechanisms controlling antigen transfer have not been well characterized, and the factors affecting this process remain elusive. We suspected that ectopic expression of CTLA-4 from mTECs might also impair the self-antigen transfer in Aire-KO, thereby also contributing to reduced Treg production. We tested this idea using a Y-Ae mAb that recognizes the Eα peptide derived from MHC-II (I-E^d) of the BALB/c mouse strain (BALB) that is complexed with MHC-II (I-A^b) from the C57BL/6 strain (B6) (Rudensky et al., 1991). When BM chimeras were generated by transferring BM cells from wild-type B6 into wild-type BALB (WT/B6 into WT/BALB), Y-Ae-reactive DCs (Y-Ae^+ DCs) were detectable (Figure 6A), indicating that host mTEC-derived Eα peptide was obtained and presented by the donor DCs (i.e., CD8α^+ DC and Sirpα^+ DC) of B6 origin. This phenomenon of self-antigen transfer was confined to thymic DCs, and not to splenic DCs, in the BM chimeras (Figure 6B) because the spleen had no stromal component expressing high levels of MHC-II (I-E^d), unlike mTECs. When we examined the degree of self-antigen transfer using Aire-KO as recipients (WT/B6 into Aire-KO/BALB), Y-Ae^+ DCs were reduced for CD8α^+ DCs compared with those from WT recipients (WT/B6 into WT/BALB) (Figure 6A). Thymic stroma- and Aire-dependent self-antigen transfer was also observed for Sirpα^+ DCs, although it was evident only when BM cells from Aire-KO, but not WT, were used for the transfer with limited numbers of the animals so far analyzed (Figure 6A, right; compare red and black columns). In contrast, we observed no obvious change in the Y-Ae^+ DCs (CD8α^+ DCs and Sirpα^+ DCs) irrespective of whether the BM cells were from WT or Aire-KO (Figure 6A), suggesting that Aire in thymic stroma controls self-antigen transfer in this experimental system.

We then examined whether impaired self-antigen transfer in the Aire-KO thymic microenvironment might be associated with the aberrant expression of CTLA-4 from Aire-KO mTECs. For this purpose, we injected CTLA-4 Ig into the BM chimeras (i.e., WT/B6 into WT/BALB) to reduce the availability of CD80/CD86 ligands from wild-type BM-APCs, mimicking the condition where the aberrant expression of CTLA-4 from Aire-KO mTECs captured the CD80/CD86 ligands on BM-APCs: the same treatment resulted in the reduced production of Tregs in WT as described above (Figure 5B). We found that Y-Ae^+ CD8α^+ DCs but not Y-Ae^+ Sirpα^+ DCs were reduced after capturing the CD80/CD86 ligands with CTLA-4 Ig (Figure 6C). Together, our data suggested that CTLA-4 ectopically expressed from Aire-KO mTECs impaired the production of Tregs by attenuating the agonistic TCR stimuli as a result of the impaired self-antigen transfer and with the reduced CD28 signals, as illustrated in Figure S4.

Aberrant CTLA-4 expression from Aire-deficient mTECs contributes to the development of organ-specific autoimmunity

Finally, we examined the contribution of ectopically expressed CTLA-4 from Aire-KO mTECs to the development of the organ-specific autoimmune disease by the thymus graft experiment (Figure 7A). Grafting the embryonic thymi from WT induced low-grade inflammatory lesions in the salivary gland, liver, lung, and kidney, possibly due to homeostatic expansion of autoimmune-prone T cells in the hosts in this experimental setting (Figure 7B); pathological changes of the four organs (i.e., salivary gland, kidney, liver, and lung) were scored and summed for an individual mouse as "disease score" (Figure S5A). Grafting of thymi from Aire-KO resulted in significantly more severe autoimmune lesions than did the use of control grafts (Figure 7B; representative results are shown in Figure 7C). Of note, grafting the thymi lacking both Aire and CTLA-4 (Figure 7D) resulted in significantly milder pathological changes compared with the Aire-KO thymic grafts, which was comparable to those induced by grafting of WT thymi (Figures 7B and 7C). Alternatively, when pathological changes of each organ were evaluated (Figure S5A), we observed significant improvement in the salivary gland and kidney but not in the liver and lung from the Aire/CTLA-4-dKO group compared with the Aire-KO group (Figure S5B). We also found that the recipients of thymus grafts lacking both Aire and CTLA-4 produced significantly lower levels of autoantibodies against the stomach compared with the Aire-KO thymic grafts (Figure 7E). Taken together, the results suggested that aberrant expression of CTLA-4 from Aire-KO mTECs, at least in part, contributes to the development of Aire-dependent autoimmunity although other factors such as altered expression of TRAs and/or chemokines (e.g., Ccl25) from Aire-KO mTECs might be also responsible for the disease (Nishijima et al., 2022).

DISCUSSION

Our study has revealed a unique role of Aire in the suppression of disfavored CTLA-4 expression from mTECs to prevent autoimmunity. Because CTLA-4 is involved in Treg-mediated physiological immune suppression in peripheral tolerance (Qureshi et al., 2011; Tekguc et al., 2021; Walker and Sansom, 2011; Wing et al., 2008), it is interesting to note that the same CTLA-4 molecule is responsible for the autoimmunity if it is ectopically expressed from the thymic stroma. In this regard, the overall ability of Aire-KO mTECs to limit the availability of CTLA-4 ligands from DCs is unknown when compared with that of Tregs on a per-cell basis. However, given that the thymic medulla is a rather compact three-dimensional structure where thymic DCs and Aire-expressing mTECs reside in close contact, the total number of mTECs expressing CTLA-4 must be sufficient to modulate the function of DCs. This notion was supported by the reduced expression level of CTLA-4 ligands on thymic DCs from Aire-KO. However, it would

(C) Percentages and numbers of thymic Tregs and Treg precursors in Aire/CTLA-4-dKO. Neonatal mice at the age of 9 days were analyzed. Data were pooled from more than four independent experiments ($n = 10$ for WT, $n = 8$ for Aire-KO, $n = 7$ for CTLA-4-KO, and $n = 5$ for Aire/CTLA-4-dKO). Representative profiles of flow cytometry are shown on the left. Bars indicate means ± SD. Significances were determined using unpaired two-tailed Student's t test (A and B) or one-way ANOVA coupled with Tukey's multiple comparison test (C). *$p < 0.05$, **$p < 0.01$, ***$p < 0.005$; n.s., not significant. See also Figure S3.

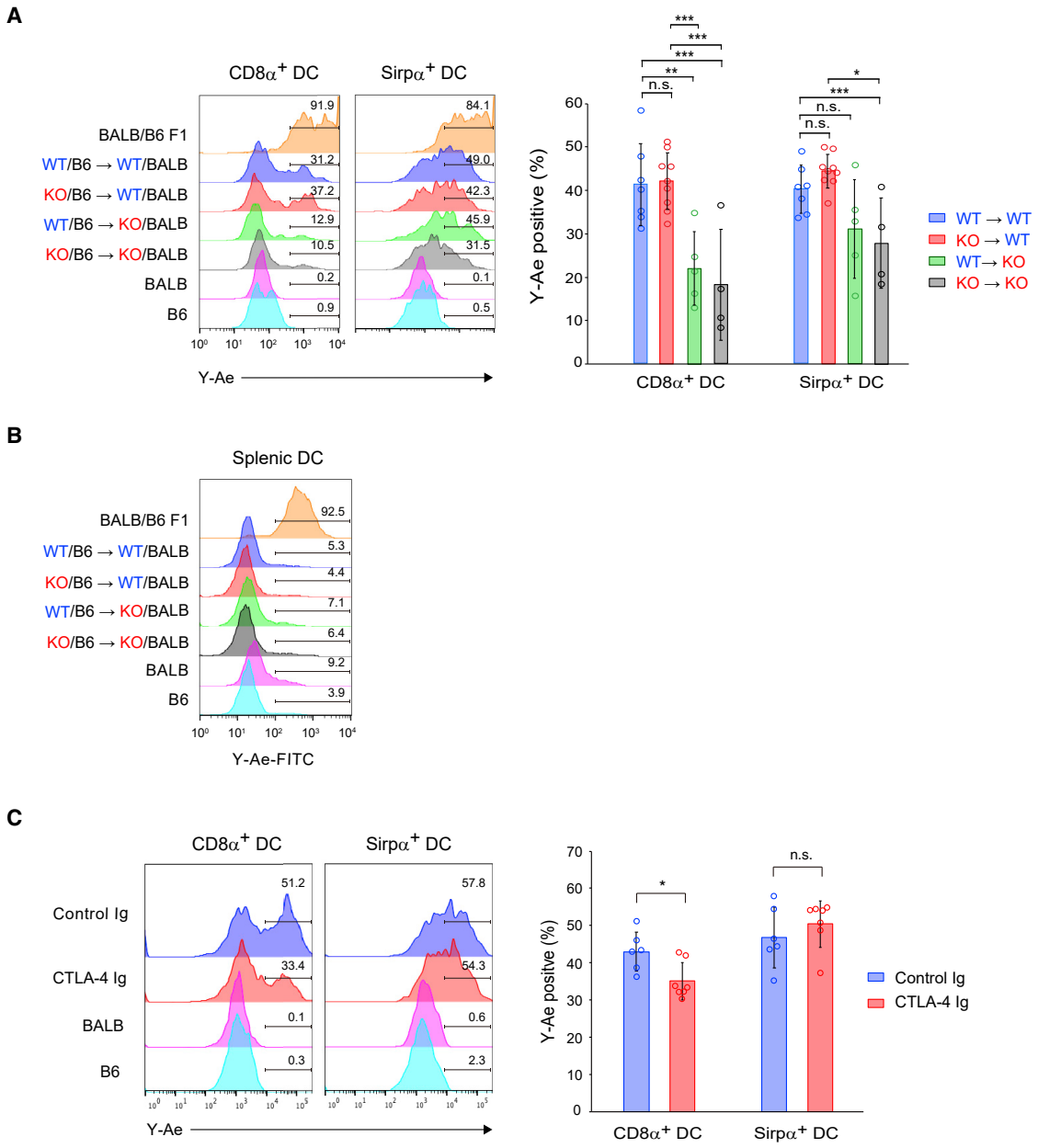

Figure 6. Blocking the CD80/CD86-CD28 signals attenuates the self-antigen transfer

(A and B) Detection of Y-Ae$^+$ cells from CD8α$^+$ DCs and Sirpα$^+$ DCs in the thymus (A) and from CD11c$^+$ DCs in the spleen (B) from various BM chimeras. Cells from untreated F_1 mice were produced by crossing WT on BALB with WT on B6 (BALB/B6 F1). WT (BALB) and WT (B6) served as controls for the staining. Data were pooled from three independent experiments ($n = 7$ for WT → WT, $n = 9$ for KO → WT, $n = 5$ for WT → KO, and $n = 4$ for KO → KO). One representative result is shown on the left. Bars indicate means ± SD.

(C) Detection of Y-Ae$^+$ cells from CD8α$^+$ DCs and Sirpα$^+$ DCs from the BM chimeras (WT/B6 into WT/BALB) after injection with CTLA-4/human IgG Fc fusion protein (CTLA-4 Ig). Human IgG (Control Ig) was injected as a control ($n = 6$ for Control Ig and $n = 7$ for CTLA-4 Ig). One representative result is shown on the left. Bars indicate means ± SD. Significances were determined using unpaired two-tailed Student's t test (C) or one-way ANOVA coupled with Tukey's multiple comparison test (A). *p < 0.05, **p < 0.01, ***p < 0.005; n.s., not significant. See also Figure S4.

also be important to mention that the degree of the reduction of CTLA-4 ligand expression from thymic DCs in Aire-KO using anti-CD86 mAb or rCTLA-4 as a probe was rather small (Figure 4C) compared with the clear interaction between recombinant CD80/CD86 and CTLA-4-expressing mTECs assessed *in vitro* (Figure 3). This is most likely because our flow-cytometric analysis for the expression of CTLA-4 ligands was performed using whole thymic DCs irrespective of their relative location to the CTLA-4-expressing mTECs despite the fact that trans-endocytosis takes place by the cell-to-cell contact *in situ*.

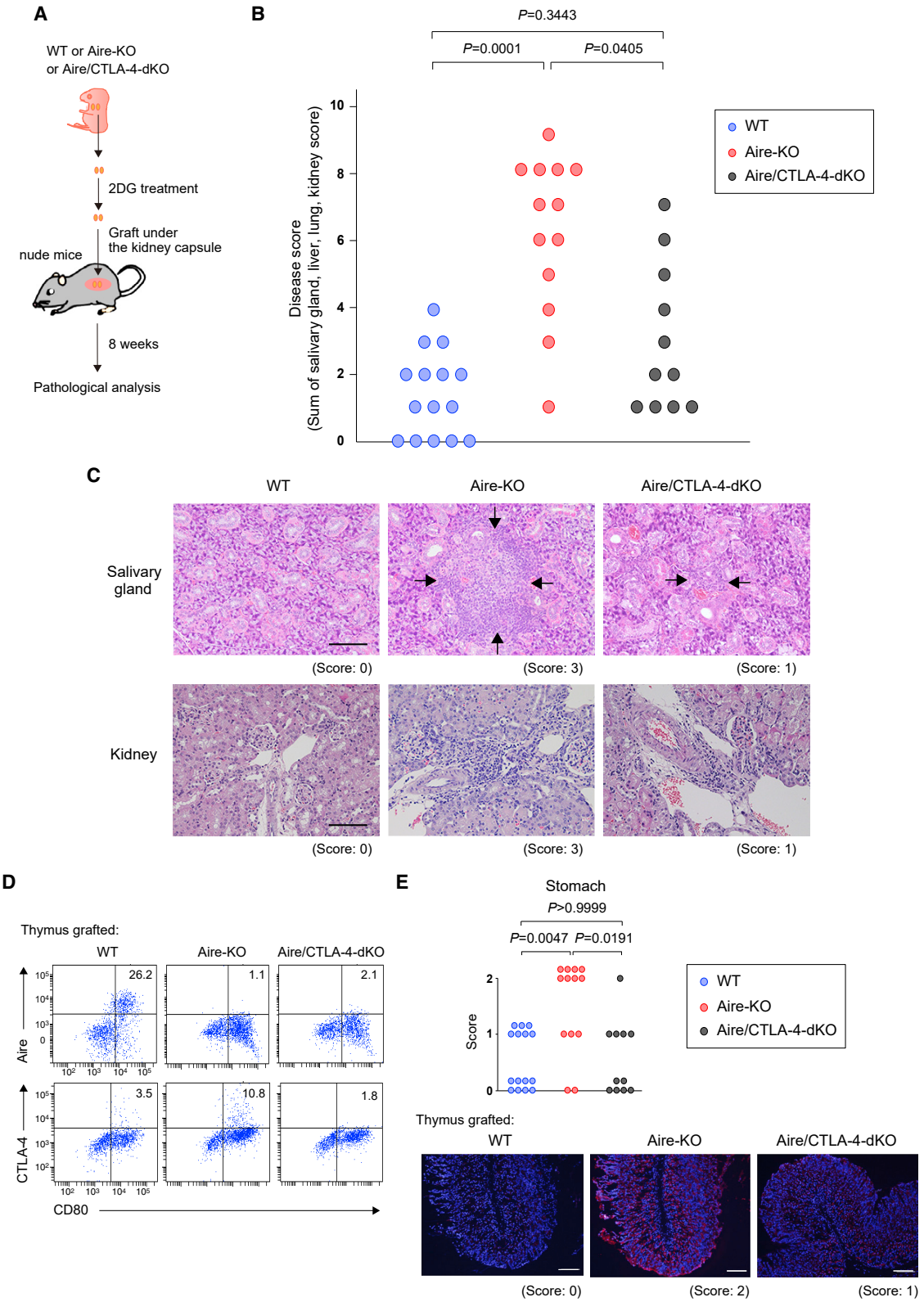

(legend on next page)

We have demonstrated, using scRNA sequencing analyses, that aberrant expression of CTLA-4 from Aire-KO mTECs was due to the altered heterogeneity of mTECs. Of note, similar mechanisms applied to the reduced expression of many TRAs from Aire-KO mTECs (Nishijima et al., 2022). Thus, altered heterogeneity of mTECs affects not only expression levels of promiscuously expressed TRA genes but also the expression of the immunologically important molecule(s) such as CTLA-4 as demonstrated in the current study. The exact Aire's target(s) that control(s) the differentiation program of mTECs await(s) further study.

We, in the present study, and others have demonstrated that Aire in thymic stroma controls the self-antigen transfer (Hubert et al., 2011; Leventhal et al., 2016; Perry et al., 2018). However, the exact molecular mechanisms controlling this process remained unclear. Our discovery of the ectopic expression of CTLA-4 from Aire-KO mTECs has brought a novel insight into this puzzle: reducing the co-stimulatory signals through CD28 by the ectopic CTLA-4 expression from Aire-KO mTECs attenuated the self-antigen transfer from mTECs to thymic DCs assessed with a peptide-in-groove mAb Y-Ae (Rudensky et al., 1991). Because transcription of MHC-II (I-E^d) from mTECs is not controlled by Aire (Kuroda et al., 2005), the reduction of Y-Ae^+ cells was not due to the altered Eα expression from Aire-KO mTECs. Similarly, because the half-life of mTECs was not different between WT and Aire-KO (Nishikawa et al., 2014), altered uptake of mTEC debris by DCs in Aire deficiency is an unlikely explanation for the reduced antigen transfer. Altered trogocytosis (Nakayama, 2014) and the secretion of mTEC-derived exosomes (Skogberg et al., 2015) might also be involved in the defective antigen transfer, although neither has been demonstrated to be Aire dependent so far. Thus, how the reduced CD28 signals on thymic DCs resulted in the attenuated self-antigen transfer and the exact mechanisms controlling antigen transfer more generally need to be explored.

It would also be important to know which thymic DC populations were affected by the lack of Aire for self-antigen transfer. One study suggested that CD8α^+ DCs play a crucial role in the antigen transfer via scavenger receptor CD36 (Perry et al., 2018) and Batf3-deficient mice showed the defect in this pathway (Perry et al., 2014) because the development of CD8α^+ DCs is dependent on Batf3 (Murphy et al., 2016). In contrast, Leventhal et al. reported that Batf3-dependent CD8α^+ DCs were dispensable for the self-antigen transfer-mediated Treg production. They suggested that both CD8α^+ and Sirpα^+ DCs have a redundant role in this action (Leventhal et al., 2016). In Aire-KO, both CD8α^+ and Sirpα^+ DCs showed impaired antigen transfer when it was assessed with Y-Ae mAb (compare red and black columns for Sirpα^+ DCs in Figure 6A, right). Consistent with this finding, expression levels of CTLA-4 ligands detected by both anti-CD86 mAb and rCTLA-4 as probes were reduced in both P2 (CD8α^+ DC) and P3 (Sirpα^+ DC) populations in Aire-KO (Figure 4C). Thus, we suggest that both CD8α^+ DCs and Sirpα^+ DCs are involved in the Aire-dependent autoimmune process. In contrast to this view, however, injection of CTLA-4 Ig into the BM chimeras resulted in the reduced Y-Ae expression only from CD8α^+ DCs and not from Sirpα^+ DCs (Figure 6C). One possible explanation for this discrepancy is that the effect of injection of CTLA-4 Ig into BM chimeras may not be as robust as that of abnormally expressed CTLA-4 from Aire-KO mTECs; the former may only mask the CTLA-4 ligands, whereas the latter can additionally remove the CTLA-4 ligands through trans-endocytosis (Qureshi et al., 2011; Walker and Sansom, 2011). The differential duration of the action between injection of CTLA-4 Ig and continuous CTLA-4 expression from Aire-KO mTECs may also account for the gap.

Both Aire-KO and injection of CTLA-4 Ig into WT showed the reduced numbers of mature $CD25^+Foxp3^+$ Tregs together with $CD25^-Foxp3^+$ Treg precursors. Recently, two distinct types of Treg precursors have been reported: $CD25^+Foxp3^-$ and $CD25^-Foxp3^{+/low}$ Treg precursors, and the development of each Treg precursor was controlled by distinct signaling pathways (Owen et al., 2019). Because only $CD25^-Foxp3^+$ Treg precursors but not $CD25^+Foxp3^-$ Treg precursors were affected in Aire-KO and in WT injected with CTLA-4 Ig, we speculate that $CD25^-Foxp3^{+/low}$ Treg precursors rely more on the positive CD28 signals compared with $CD25^+Foxp3^-$ Treg precursors. Consistent with this hypothesis, it was reported that $CD25^-Foxp3^{+/low}$ Treg precursors arose by co-opting positive-selection programs (i.e., genes that enhance signaling via TCR and sensitivity to IL-2) rather than negative-selection programs (i.e., pro-apoptotic genes and genes involved in negative selection) (Owen et al., 2019).

We focused on the effect of the aberrant expression of CTLA-4 from Aire-KO mTECs on the production of Tregs but not the negative selection in the present study. Because Treg production and negative selection are interconnected events (Sakaguchi et al., 2020) both affected by Aire (Anderson et al., 2005;

Figure 7. Aberrant CTLA-4 expression from Aire-deficient mTECs contributes to the development of organ-specific autoimmunity

(A) Schematic representation of the graft of fetal thymi. Fetal thymi from WT, Aire-KO, or Aire/CTLA-4-dKO were grafted under the kidney capsule of nude mice. The mice were analyzed 8 weeks after the graft.

(B) Pathological scores for the organs from nude mice engrafted with fetal thymi from WT (n = 15), Aire-KO (n = 13), and Aire/CTLA-4-dKO (n = 11). Pathological scores for the organs were graded as none (score 0), mild (score 1), moderate (score 2), and severe (score 3). One circle corresponds to one mouse analyzed in which the pathological changes of four organs (salivary gland, kidney, liver, and lung) were summed for an individual mouse as shown in Figure S5A.

(C) Representative salivary gland and kidney pathologies with the corresponding scores. Arrows indicate lymphoid cell infiltrations. Scale bar: 100 μm.

(D) Flow-cytometric analysis of the expression of CTLA-4 and Aire together with CD80 in mTECs isolated from grafted thymi. Plots were gated for $CD45^-EpCAM^+UEA\text{-}1^+$ cells. Representative profiles of flow cytometry are shown.

(E) Production of autoantibody against the stomach in nude mice engrafted with thymi from WT (n = 15), Aire-KO (n = 13), and Aire/CTLA-4-dKO (n = 11). Reactivities were graded as none (score 0), moderate (score 1), and strong (score 2). Representative reactivities with the corresponding scores are shown at the bottom. Scale bar: 100 μm.

p values were computed using Dunn's Kruskal-Wallis multiple comparisons tests in GraphPad Prism for the comparison of non-parametric pathological scores (B and E). See also Figure S5.

Mouri et al., 2017) and because DCs play an important role in the thymic tolerance induction (Klein et al., 2014; Proekt et al., 2017), aberrant expression of CTLA-4 from Aire-KO mTECs may have an impact on the negative-selection process as well. However, the fact that simultaneous depletion of Aire and CTLA-4 resulted in the amelioration of organ-specific autoimmunity, which was strongly associated with the rescue of Treg production, suggested that altered production of Tregs has a critical role for the autoimmune pathogenesis in Aire-KO, as suggested for AIRE-deficient patients (Hetemaki et al., 2016; Kekalainen et al., 2007; Laakso et al., 2010; Ryan et al., 2005). Interestingly, it has recently been reported that motifs of the CD28 cytoplasmic domain required for negative selection and Treg production are different. The differential requirement of CD28 depending on the APC types was also noted (Watanabe et al., 2020). Although our present study may shed light on the CD28-mediated central tolerance mechanisms from a novel viewpoint, more studies are required to define the relative contribution of the defect in Treg production and the impaired negative selection to the development of Aire-dependent autoimmunity.

It would also be important to determine the extent to which each causal mechanism so far proposed, i.e., altered expression of TRAs from mTECs, altered expression of chemokines from mTECs (Laan et al., 2009), altered function of thymic DCs proposed in the present study, or each combined, play a role for the development of organ-specific autoimmunity in Aire deficiency. The significance of the ectopic expression of CTLA-4 in Aire-dependent autoimmunity was underscored by the fact that impaired production of Tregs in Aire-KO was rescued by the simultaneous depletion of CTLA-4 expression. Of note, this recovery of the Tregs and accompanied amelioration of autoimmunity took place despite the fact that the expression of several prototypic Aire-dependent TRAs remained low in Aire/CTLA-4 double-KO mTECs as in Aire-KO mTECs. To exactly answer how Aire establishes self-tolerance in the thymus, Aire's primary target gene(s) need(s) to be defined among many genes controlled by Aire directly or indirectly.

In conclusion, we have demonstrated that one important mechanism responsible for the development of Aire-dependent autoimmunity was the altered function of thymic DCs due to the aberrant expression of CTLA-4 from mTECs (Figure S3D). Modulation of the CTLA-4 ligands on thymic DCs by Aire-KO mTECs not only impaired the ability of DCs to provide co-stimulatory signals but also attenuated self-antigen transfer between DCs and mTECs, both required for the production of Tregs. Thus, strategies to target the ectopic CTLA-4 expression from mTECs might be a novel therapeutic approach to ameliorate Aire-dependent autoimmunity.

Limitations of the study

Although we have suggested that mTEC-intrinsic ectopic expression of CTLA-4 contributes to the Aire-dependent autoimmunity, we have not approached this by analyzing a strain in which CTLA-4 is specifically depleted in Aire-deficient mTECs, i.e., CTLA-4-floxed mice crossed with a Foxn1-Cre strain on the Aire-deficient background. Furthermore, we have not explored additional Aire-dependent autoimmune mechanisms in the periphery (Matsumoto et al., 2020) besides the control of TRA expression by extra-thymic Aire-expressing cells.

STAR★METHODS

Detailed methods are provided in the online version of this paper and include the following:

- KEY RESOURCES TABLE
- RESOURCE AVAILABILITY
  - Lead contact
  - Materials availability
  - Data and code availability
- EXPERIMENTAL MODEL AND SUBJECT DETAILS
  - Mice
- METHOD DETAILS
  - Thymic epithelial cell preparation
  - Flow cytometric analysis
  - Single-cell (sc) RNA-seq analysis
  - *In vitro* endocytosis assay
  - *Ex vivo* endocytosis assay
  - Immunohistochemistry
  - Immunocytochemical analysis
  - Reaggregate thymic organ culture
  - Bone marrow transfer
  - *In vivo* mouse treatment
  - Real-time PCR
  - Thymus graft
  - Pathology
  - Detection of autoantibodies
- QUANTIFICATION AND STATISTICAL ANALYSIS

SUPPLEMENTAL INFORMATION

Supplemental information can be found online at https://doi.org/10.1016/j.celrep.2022.110384.

ACKNOWLEDGMENTS

We thank Drs. Y. Nishikawa and S. Chikuma for helpful discussion. We also thank Ms. F. Hirota for technical assistance. This work was supported in part by JSPS KAKENHI Grant Numbers 16H06496, 16K21731, 18K19564, and 19H03699 (to Mitsuru Matsumoto) and 19K07626 (to J.M.).

AUTHOR CONTRIBUTIONS

J.M. and Mitsuru Matsumoto designed the experiments. J.M., Minoru Matsumoto, R.M., and Mitsuru Matsumoto conducted the experiments. Minoru Matsumoto and K.T. evaluated the pathological changes in mice. J.M., Minoru Matsumoto, H.Y., and Mitsuru Matsumoto analyzed the data and wrote the paper.

DECLARATION OF INTERESTS

The authors declare no competing interests.

Received: February 10, 2021
Revised: June 8, 2021
Accepted: January 24, 2022
Published: February 15, 2022

REFERENCES

Anderson, M.S., Venanzi, E.S., Chen, Z., Berzins, S.P., Benoist, C., and Mathis, D. (2005). The cellular mechanism of aire control of T cell tolerance. Immunity *23*, 227–239.

Anderson, M.S., Venanzi, E.S., Klein, L., Chen, Z., Berzins, S.P., Turley, S.J., von Boehmer, H., Bronson, R., Dierich, A., Benoist, C., and Mathis, D. (2002). Projection of an immunological self shadow within the thymus by the aire protein. Science *298*, 1395–1401.

Aschenbrenner, K., D'Cruz, L.M., Vollmann, E.H., Hinterberger, M., Emmerich, J., Swee, L.K., Rolink, A., and Klein, L. (2007). Selection of Foxp3+ regulatory T cells specific for self antigen expressed and presented by Aire+ medullary thymic epithelial cells. Nat. Immunol. *8*, 351–358.

Cowan, J.E., Baik, S., McCarthy, N.I., Parnell, S.M., White, A.J., Jenkinson, W.E., and Anderson, G. (2018). Aire controls the recirculation of murine Foxp3(+) regulatory T-cells back to the thymus. Eur. J. Immunol. *48*, 844–854.

Hetemaki, I., Jarva, H., Kluger, N., Baldauf, H.M., Laakso, S., Bratland, E., Husebye, E.S., Kisand, K., Ranki, A., Peterson, P., and Arstila, T.P. (2016). Anti-commensal responses are associated with regulatory T cell defect in autoimmune polyendocrinopathy-candidiasis-ectodermal dystrophy patients. J. Immunol. *196*, 2955–2964.

Hubert, F.X., Kinkel, S.A., Davey, G.M., Phipson, B., Mueller, S.N., Liston, A., Proietto, A.I., Cannon, P.Z., Forehan, S., Smyth, G.K., et al. (2011). Aire regulates the transfer of antigen from mTECs to dendritic cells for induction of thymic tolerance. Blood *118*, 2462–2472.

Inglesfield, S., Cosway, E.J., Jenkinson, W.E., and Anderson, G. (2019). Rethinking thymic tolerance: lessons from mice. Trends Immunol. *40*, 279–291.

Jung, S., Unutmaz, D., Wong, P., Sano, G., De los Santos, K., Sparwasser, T., Wu, S., Vuthoori, S., Ko, K., Zavala, F., et al. (2002). In vivo depletion of CD11c+ dendritic cells abrogates priming of CD8+ T cells by exogenous cell-associated antigens. Immunity *17*, 211–220.

Kawano, H., Nishijima, H., Morimoto, J., Hirota, F., Morita, R., Mouri, Y., Nishioka, Y., and Matsumoto, M. (2015). Aire expression is inherent to most medullary thymic epithelial cells during their differentiation program. J. Immunol. *195*, 5149–5158.

Kekalainen, E., Tuovinen, H., Joensuu, J., Gylling, M., Franssila, R., Pontynen, N., Talvensaari, K., Perheentupa, J., Miettinen, A., and Arstila, T.P. (2007). A defect of regulatory T cells in patients with autoimmune polyendocrinopathy-candidiasis-ectodermal dystrophy. J. Immunol. *178*, 1208–1215.

Klein, L., Kyewski, B., Allen, P.M., and Hogquist, K.A. (2014). Positive and negative selection of the T cell repertoire: what thymocytes see (and don't see). Nat. Rev. Immunol. *14*, 377–391.

Koble, C., and Kyewski, B. (2009). The thymic medulla: a unique microenvironment for intercellular self-antigen transfer. J. Exp. Med. *206*, 1505–1513.

Kuroda, N., Mitani, T., Takeda, N., Ishimaru, N., Arakaki, R., Hayashi, Y., Bando, Y., Izumi, K., Takahashi, T., Nomura, T., et al. (2005). Development of autoimmunity against transcriptionally unrepressed target antigen in the thymus of aire-deficient mice. J. Immunol. *174*, 1862–1870.

Kyewski, B., and Klein, L. (2006). A central role for central tolerance. Annu. Rev. Immunol. *24*, 571–606.

Laakso, S.M., Laurinolli, T.T., Rossi, L.H., Lehtoviita, A., Sairanen, H., Perheentupa, J., Kekalainen, E., and Arstila, T.P. (2010). Regulatory T cell defect in APECED patients is associated with loss of naive FOXP3(+) precursors and impaired activated population. J. Autoimmun. *35*, 351–357.

Laan, M., Kisand, K., Kont, V., Moll, K., Tserel, L., Scott, H.S., and Peterson, P. (2009). Autoimmune regulator deficiency results in decreased expression of CCR4 and CCR7 ligands and in delayed migration of CD4+ thymocytes. J. Immunol. *183*, 7682–7691.

Leventhal, D.S., Gilmore, D.C., Berger, J.M., Nishi, S., Lee, V., Malchow, S., Kline, D.E., Kline, J., Vander Griend, D.J., Huang, H., et al. (2016). Dendritic cells coordinate the development and homeostasis of organ-specific regulatory T cells. Immunity *44*, 847–859.

Li, M.O., and Rudensky, A.Y. (2016). T cell receptor signalling in the control of regulatory T cell differentiation and function. Nat. Rev. Immunol. *16*, 220–233.

Linsley, P.S., Bradshaw, J., Greene, J., Peach, R., Bennett, K.L., and Mittler, R.S. (1996). Intracellular trafficking of CTLA-4 and focal localization towards sites of TCR engagement. Immunity *4*, 535–543.

Luhder, F., Chambers, C., Allison, J.P., Benoist, C., and Mathis, D. (2000). Pinpointing when T cell costimulatory receptor CTLA-4 must be engaged to dampen diabetogenic T cells. Proc. Natl. Acad. Sci. U S A *97*, 12204–12209.

Malchow, S., Leventhal, D.S., Lee, V., Nishi, S., Socci, N.D., and Savage, P.A. (2016). Aire enforces immune tolerance by directing autoreactive T cells into the regulatory T cell lineage. Immunity *44*, 1102–1113.

Marangoni, F., Zhakyp, A., Corsini, M., Geels, S.N., Carrizosa, E., Thelen, M., Mani, V., Prussmann, J.N., Warner, R.D., Ozga, A.J., et al. (2021). Expansion of tumor-associated Treg cells upon disruption of a CTLA-4-dependent feedback loop. Cell *184*, 3998–4015.e19.

Mathis, D., and Benoist, C. (2009). Aire. Annu. Rev. Immunol. *27*, 287–312.

Matsumoto, M., Tsuneyama, K., Morimoto, J., Hosomichi, K., Matsumoto, M., and Nishijima, H. (2020). Tissue-specific autoimmunity controlled by aire in thymic and peripheral tolerance mechanisms. Int. Immunol. *32*, 117–131.

Morimoto, J., Nishikawa, Y., Kakimoto, T., Furutani, K., Kihara, N., Matsumoto, M., Tsuneyama, K., Kozono, Y., Kozono, H., Hozumi, K., et al. (2018). Aire controls in trans the production of medullary thymic epithelial cells expressing ly-6C/Ly-6G. J. Immunol. *201*, 3244–3257.

Mouri, Y., Ueda, Y., Yamano, T., Matsumoto, M., Tsuneyama, K., Kinashi, T., and Matsumoto, M. (2017). Mode of tolerance induction and requirement for aire are governed by the cell types that express self-antigen and those that present antigen. J. Immunol. *199*, 3959–3971.

Murphy, T.L., Grajales-Reyes, G.E., Wu, X., Tussiwand, R., Briseno, C.G., Iwata, A., Kretzer, N.M., Durai, V., and Murphy, K.M. (2016). Transcriptional control of dendritic cell development. Annu. Rev. Immunol. *34*, 93–119.

Nakayama, M. (2014). Antigen presentation by MHC-dressed cells. Front. Immunol. *5*, 672.

Niki, S., Oshikawa, K., Mouri, Y., Hirota, F., Matsushima, A., Yano, M., Han, H., Bando, Y., Izumi, K., Matsumoto, M., et al. (2006). Alteration of intra-pancreatic target-organ specificity by abrogation of aire in NOD mice. J. Clin. Invest. *116*, 1292–1301.

Nishijima, H., Matsumoto, M., Morimoto, J., Hosomichi, K., Akiyama, N., Akiyama, T., Oya, T., Tsuneyama, K., Yoshida, H., and Matsumoto, M. (2022). Aire controls heterogeneity of medullary thymic epithelial cells for the expression of self-antigens. J. Immunol. *208*, 303–320.

Nishikawa, Y., Hirota, F., Yano, M., Kitajima, H., Miyazaki, J., Kawamoto, H., Mouri, Y., and Matsumoto, M. (2010). Biphasic aire expression in early embryos and in medullary thymic epithelial cells before end-stage terminal differentiation. J. Exp. Med. *207*, 963–971.

Nishikawa, Y., Nishijima, H., Matsumoto, M., Morimoto, J., Hirota, F., Takahashi, S., Luche, H., Fehling, H.J., Mouri, Y., and Matsumoto, M. (2014). Temporal lineage tracing of aire-expressing cells reveals a requirement for aire in their maturation program. J. Immunol. *192*, 2585–2592.

Owen, D.L., Mahmud, S.A., Sjaastad, L.E., Williams, J.B., Spanier, J.A., Simeonov, D.R., Ruscher, R., Huang, W., Proekt, I., Miller, C.N., et al. (2019). Thymic regulatory T cells arise via two distinct developmental programs. Nat. Immunol. *20*, 195–205.

Perry, J.S.A., Lio, C.J., Kau, A.L., Nutsch, K., Yang, Z., Gordon, J.I., Murphy, K.M., and Hsieh, C.S. (2014). Distinct contributions of aire and antigen-presenting-cell subsets to the generation of self-tolerance in the thymus. Immunity *41*, 414–426.

Perry, J.S.A., Russler-Germain, E.V., Zhou, Y.W., Purtha, W., Cooper, M.L., Choi, J., Schroeder, M.A., Salazar, V., Egawa, T., Lee, B.C., et al. (2018). Transfer of cell-surface antigens by scavenger receptor CD36 promotes thymic regulatory T cell receptor repertoire development and allo-tolerance. Immunity *48*, 1271.

Proekt, I., Miller, C.N., Lionakis, M.S., and Anderson, M.S. (2017). Insights into immune tolerance from AIRE deficiency. Curr. Opin. Immunol. *49*, 71–78.

Qureshi, O.S., Zheng, Y., Nakamura, K., Attridge, K., Manzotti, C., Schmidt, E.M., Baker, J., Jeffery, L.E., Kaur, S., Briggs, Z., et al. (2011). Trans-endocytosis of CD80 and CD86: a molecular basis for the cell-extrinsic function of CTLA-4. Science *332*, 600–603.

Rudensky, A., Rath, S., Preston-Hurlburt, P., Murphy, D.B., and Janeway, C.A., Jr. (1991). On the complexity of self. Nature *353*, 660–662.

Ryan, K.R., Lawson, C.A., Lorenzi, A.R., Arkwright, P.D., Isaacs, J.D., and Lilic, D. (2005). CD4+CD25+ T-regulatory cells are decreased in patients with autoimmune polyendocrinopathy candidiasis ectodermal dystrophy. J. Allergy Clin. Immunol. *116*, 1158–1159.

Sakaguchi, S., Mikami, N., Wing, J.B., Tanaka, A., Ichiyama, K., and Ohkura, N. (2020). Regulatory T cells and human disease. Annu. Rev. Immunol. *38*, 541–566.

Salomon, B., Lenschow, D.J., Rhee, L., Ashourian, N., Singh, B., Sharpe, A., and Bluestone, J.A. (2000). B7/CD28 costimulation is essential for the homeostasis of the CD4+CD25+ immunoregulatory T cells that control autoimmune diabetes. Immunity *12*, 431–440.

Sansom, S.N., Shikama-Dorn, N., Zhanybekova, S., Nusspaumer, G., Macaulay, I.C., Deadman, M.E., Heger, A., Ponting, C.P., and Hollander, G.A. (2014). Population and single-cell genomics reveal the aire dependency, relief from Polycomb silencing, and distribution of self-antigen expression in thymic epithelia. Genome Res. *24*, 1918–1931.

Skogberg, G., Telemo, E., and Ekwall, O. (2015). Exosomes in the thymus: antigen transfer and vesicles. Front. Immunol. *6*, 366.

Smigiel, K.S., Richards, E., Srivastava, S., Thomas, K.R., Dudda, J.C., Klonowski, K.D., and Campbell, D.J. (2014). CCR7 provides localized access to IL-2 and defines homeostatically distinct regulatory T cell subsets. J. Exp. Med. *211*, 121–136.

Sonkoly, E., Janson, P., Majuri, M.L., Savinko, T., Fyhrquist, N., Eidsmo, L., Xu, N., Meisgen, F., Wei, T., Bradley, M., et al. (2010). MiR-155 is overexpressed in patients with atopic dermatitis and modulates T-cell proliferative responses by targeting cytotoxic T lymphocyte-associated antigen 4. J. Allergy Clin. Immunol. *126*, 581–589.e1-20.

Stuart, T., Butler, A., Hoffman, P., Hafemeister, C., Papalexi, E., Mauck, W.M., 3rd, Hao, Y., Stoeckius, M., Smibert, P., and Satija, R. (2019). Comprehensive integration of single-cell data. Cell *177*, 1888–1902 e1821.

Sugiura, D., Maruhashi, T., Okazaki, I.M., Shimizu, K., Maeda, T.K., Takemoto, T., and Okazaki, T. (2019). Restriction of PD-1 function by cis-PD-L1/CD80 interactions is required for optimal T cell responses. Science *364*, 558–566.

Tai, X., Cowan, M., Feigenbaum, L., and Singer, A. (2005). CD28 costimulation of developing thymocytes induces Foxp3 expression and regulatory T cell differentiation independently of interleukin 2. Nat. Immunol. *6*, 152–162.

Tai, X., Erman, B., Alag, A., Mu, J., Kimura, M., Katz, G., Guinter, T., McCaughtry, T., Etzensperger, R., Feigenbaum, L., et al. (2013). Foxp3 transcription factor is proapoptotic and lethal to developing regulatory T cells unless counterbalanced by cytokine survival signals. Immunity *38*, 1116–1128.

Teft, W.A., Kirchhof, M.G., and Madrenas, J. (2006). A molecular perspective of CTLA-4 function. Annu. Rev. Immunol. *24*, 65–97.

Tekguc, M., Wing, J.B., Osaki, M., Long, J., and Sakaguchi, S. (2021). Treg-expressed CTLA-4 depletes CD80/CD86 by trogocytosis, releasing free PD-L1 on antigen-presenting cells. Proc. Natl. Acad. Sci. U S A *118*, e2023739118.

Tomofuji, Y., Takaba, H., Suzuki, H.I., Benlaribi, R., Martinez, C.D.P., Abe, Y., Morishita, Y., Okamura, T., Taguchi, A., Kodama, T., and Takayanagi, H. (2020). Chd4 choreographs self-antigen expression for central immune tolerance. Nat. Immunol. *21*, 892–901.

Valk, E., Rudd, C.E., and Schneider, H. (2008). CTLA-4 trafficking and surface expression. Trends Immunol. *29*, 272–279.

Walker, L.S., and Sansom, D.M. (2011). The emerging role of CTLA4 as a cell-extrinsic regulator of T cell responses. Nat. Rev. Immunol. *11*, 852–863.

Watanabe, M., Lu, Y., Breen, M., and Hodes, R.J. (2020). B7-CD28 co-stimulation modulates central tolerance via thymic clonal deletion and Treg generation through distinct mechanisms. Nat. Commun. *11*, 6264.

Wing, K., Onishi, Y., Prieto-Martin, P., Yamaguchi, T., Miyara, M., Fehervari, Z., Nomura, T., and Sakaguchi, S. (2008). CTLA-4 control over Foxp3+ regulatory T cell function. Science *322*, 271–275.

Yang, S., Fujikado, N., Kolodin, D., Benoist, C., and Mathis, D. (2015). Immune tolerance. regulatory T cells generated early in life play a distinct role in maintaining self-tolerance. Science *348*, 589–594.

Yano, M., Kuroda, N., Han, H., Meguro-Horike, M., Nishikawa, Y., Kiyonari, H., Maemura, K., Yanagawa, Y., Obata, K., Takahashi, S., et al. (2008). Aire controls the differentiation program of thymic epithelial cells in the medulla for the establishment of self-tolerance. J. Exp. Med. *205*, 2827–2838.

Zhao, Y., Lee, C.K., Lin, C.H., Gassen, R.B., Xu, X., Huang, Z., Xiao, C., Bonorino, C., Lu, L.F., Bui, J.D., and Hui, E. (2019). PD-L1:CD80 Cis-Heterodimer triggers the Co-stimulatory receptor CD28 while repressing the inhibitory PD-1 and CTLA-4 pathways. Immunity *51*, 1059–1073.e59.

STAR★METHODS

KEY RESOURCES TABLE

REAGENT or RESOURCE	SOURCE	IDENTIFIER
Antibodies		
BV421 anti-mouse CD45 (clone 30-F11)	BioLegend	Cat#103134; RRID:AB_2562559
PE/Cy7 anti-mouse CD326(EpCAM) (clone G8.8)	BioLegend	Cat#118216; RRID:AB_1236471
PE anti-mouse Ly51 (clone 6C3)	BioLegend	Cat#108308; RRID:AB_313365
APC anti-mouse CD80 (clone 16-10A1)	BioLegend	Cat#104714; RRID:AB_313135
FITC anti-mouse CD80 (clone 16-10A1)	BioLegend	Cat#104706; RRID:AB_313127
APC anti-mouse CD86 (clone GL-1)	BioLegend	Cat#105012; RRID:AB_493342
PE anti-mouse CD86 (clone GL-1)	BioLegend	Cat#105008; RRID:AB_313151
APC anti-mouse H-2D^{b} (clone KH95)	BioLegend	Cat#111514; RRID:AB_2565862
PE anti-mouse H-2D^{b} (clone KH95)	BioLegend	Cat#111508; RRID:AB_313513
FITC anti-mouse Ly-6G/Ly-6C (Gr-1) (clone RB6-8C5)	BioLegend	Cat#108406; RRID:AB_313371
APC anti-mouse CTLA-4 (clone UC10-4B9)	BioLegend	Cat#106309; RRID:AB_2230158
PE anti-mouse CTLA-4 (clone UC10-4B9)	BioLegend	Cat#106305; RRID:AB_313254
PE anti-mouse CD4 (clone RM4-5)	BioLegend	Cat#100512; RRID:AB_312715
PE/Cy7 anti-mouse CD4 (clone RM4-5)	BioLegend	Cat#100528; RRID:AB_312729
Biotin anti-mouse CD4 (clone RM4-5)	BioLegend	Cat#116010; RRID:AB_2561504
APC/Cy7 anti-mouse CD8α (clone 53-6.7)	BioLegend	Cat#100714; RRID:AB_312753
APC anti-mouse CD8α (clone 53-6.7)	BioLegend	Cat#100712; RRID:AB_312751
Biotin anti-mouse CD8α (clone 53-6.7)	BioLegend	Cat#100704; RRID:AB_312743
Biotin anti-mouse CD19 (clone 6D5)	BioLegend	Cat#115504; RRID:AB_313639
APC anti-mouse CD25 (clone PC61)	BioLegend	Cat#102012; RRID:AB_312861
PE anti-mouse CD28 (clone 37.51)	BioLegend	Cat#102105; RRID:AB_312870
PE anti-mouse CD44 (clone IM7)	BioLegend	Cat#103007; RRID:AB_312958
FITC anti-mouse CD44 (clone IM7)	BioLegend	Cat#103005; RRID:AB_312956
APC anti-mouse CD103 (clone 2E7)	BioLegend	Cat#121413; RRID:AB_1227503
APC anti-mouse CD11b (clone M1/70)	BioLegend	Cat#101212; RRID:AB_312795
FITC anti-mouse CD11b (clone M1/70)	BioLegend	Cat#101206; RRID:AB_312789
PE/Cy7 anti-mouse CD11c (clone N418)	BioLegend	Cat#117318; RRID:AB_493568
Alexa Fluor 647 anti-mouse CD11c (clone N418)	BioLegend	Cat#117314; RRID:AB_492850
PE anti-mouse CD62L (clone MEL-14)	BioLegend	Cat#104408; RRID:AB_313095
Alexa Fluor 594 anti-mouse CD107a (Lamp1) (clone 1D4B)	BioLegend	Cat#121622; RRID:AB_2563965
PE anti-human IgG Fcγ (poly23980)	BioLegend	Cat#398004; RRID:AB_2820063
FITC anti-human IgG Fcγ (poly23980)	BioLegend	Cat#398006; RRID:AB_2820064
APC Armenian Hamster IgG isotype control (clone HTK888)	BioLegend	Cat#400912
APC Rat IgG2a, κ isotype control (clone RTK2758)	BioLegend	Cat#400511; RRID:AB_2814702
APC Mouse IgG2b, κ isotype control (clone MPC-11)	BioLegend	Cat#400320; RRID:AB_326500
FITC Rat IgG2b, κ isotype control (clone RTK4530)	BioLegend	Cat#400605; RRID:AB_326549
PE Syrian Hamster IgG isotype control (clone SHG-1)	BioLegend	Cat#402008
Streptavidin APC/Cy7	BioLegend	Cat#405208
PE anti-mouse Siglec-F (clone E50-2440)	BD Biosciences	Cat#562068; RRID:AB_394341
APC anti-mouse CD172a (Sirpα) (clone P84)	BD Biosciences	Cat#560106; RRID:AB_1645218
APC anti-mouse CTLA-4 (clone UC10-4F10-11)	BD Biosciences	Cat#564331; RRID:AB_2738751
Purified anti-mouse CD16/32 (clone Ab93)	BD Biosciences	Cat#567021; RRID:AB_2870010
PE Rat IgG2a, κ isotype control (clone R35-95)	BD Biosciences	Cat#553930; RRID:AB_479724

(*Continued on next page*)

Continued

REAGENT or RESOURCE	SOURCE	IDENTIFIER
APC Rat IgG1, κ isotype control (clone R3-34)	BD Biosciences	Cat#554686; RRID:AB_398577
PE anti-mouse I-A/I-E (clone M5/114.15.2)	Invitorogen	Cat#12-5321-82; RRID:AB_465928
FITC Ea52-68 peptide bound to I-Ab (Y-Ae)	Invitorogen	Cat#11-5741-82; RRID:AB_996692
FITC anti-mouse Foxp3 (clone FJK-16s)	Invitorogen	Cat#11-5773-82; RRID:AB_465243
Alexa Fluor 488 anti-human IgG	Invitorogen	Cat#A-11013; RRID:AB_2534080
Alexa Fluor 594 anti-mouse IgG	Invitorogen	Cat#A-21201; RRID:AB_2535787
Alexa Fluor 488 GFP polyclonal	Invitorogen	Cat#A-21311; RRID:AB_221477
Biotin Ulex europaeus agglutinin (UEA-1)	Vector Laboratories	Cat#B-1065; RRID:AB_2336766
Rat anti-mouse Aire (clone MM-525)	produced in our laboratory	N/A
Chemicals, peptides, and recombinant proteins		
ORENCIA (CTLA-4 Ig)	ONO PHARMACEUTICAL CO., LTD.	N/A
Venoglobulin IH 5% (Control Ig)	Japan Blood Products Organization	N/A
*InVivo*MAb anti-mouse CTLA-4	BioXCell	Cat#BE0032; RRID:AB_1107598
*InVivo*MAb Armenian hamster IgG isotype control	BioXCell	Cat#BE0260; RRID:AB_2687739
Recombinant mouse B7-2/CD86 Fc Chimera	R&D Systems	Cat#741-B2
Recombinant mouse B7-1/CD80 Fc Chimera	R&D Systems	Cat#740-B1
Recombinant mouse CTLA-4 Fc Chimera	R&D Systems	Cat#434-CT
Propidium Iodide (PI)	BioLegend	Cat#421301
Collagenase D	Roche	Cat#11088882001
Collagenase/Dispase	Roche	Cat#11097113001
DNase I recombinant, RNase-free	Roche	Cat#04716728001
2'-Deoxyguanosine monohydrate	SIGMA	Cat#D7145-1G
Diphtheria toxin	SIGMA	Cat#D0564-1MG
Critical commercial assays		
Streptavidin Particles Plus-DM	BD Biosciences	Cat#557812
RNeasy Plus Mini Kit	QIAGEN	Cat#74134
QuantiTect Probe PCR Kit	QIAGEN	Cat#204343
Sensiscript RT KIt	QIAGEN	Cat#205211
mirVana™ miRNA Isolation Kit	Thermo Fisher Scientific	Cat#AM1560
TaqMan MicroRNA Assays	Thermo Fisher Scientific	Assay ID:464539
Foxp3/Transcription Factor Staining Buffer Set	Invitrogen	Cat#00-5523-00
Deposited data		
Raw and analyzed data	NCBI	GSE155331
Experimental models: Organisms/strains		
Mouse C57BL/6J (B6)	CLEA Japan	N/A
Mouse BALB/cA (BALB/c)	CLEA Japan	N/A
Mouse BALB/c$^{nu/nu}$	CLEA Japan	N/A
Mouse Aire$^{-/-}$ (B6)	Kuroda et al., 2005	N/A
Mouse Aire$^{-/-}$ (BALB/c); B6 Aire$^{-/-}$ backcrossed with BALB/cA for >10 generations	Kuroda et al., 2005	JAX#036465
Mouse Aire/diphtheria toxin receptor (DTR)-GFP-KI (B6)	Kawano et al., 2015	JAX#036497
Mouse Aire/GFP-KI (B6)	Yano et al., 2008	JAX#036498
Mouse CD11c-DTR/GFP-Tg (B6)	The Jackson Laboratory	JAX#004509
Mouse Foxp3/EGFP-KI (B6)	The Jackson Laboratory	JAX#006772
Mouse CTLA-4$^{-/-}$ (NOD.129 (B6))	The Jackson Laboratory	JAX#005144
Mouse CTLA-4$^{-/-}$ (BALB/c); NOD.129(B6) CTLA-4$^{-/-}$ backcrossed with BALB/cA for >7 generations	backcrossed in our laboratory	N/A
Mouse CTLA-4$^{-/-}$ (B6); NOD.129(B6) CTLA-4$^{-/-}$ backcrossed with C57BL/6 for >7 generations	backcrossed in our laboratory	N/A

(*Continued on next page*)

Continued

REAGENT or RESOURCE	SOURCE	IDENTIFIER
Mouse Rag2$^{-/-}$ (B6)	The Jackson Laboratory	JAX#008449
Oligonucleotides		
Primers and Probes for RT-qPCR (see Table S2)	SIGMA GENOSYS	N/A
Software and algorithms		
GraphPad Prism	GraphPad Software	RRID:SCR_002798
FlowJo	FlowJo	RRID:SCR_008520
FACSDiva Software	BD Biosciences	RRID:SCR_001456
BZ-X810 analyzer software	Keyence	N/A
Gene Ontology (GO) enrichment analysis	R package	clusterProfiler

RESOURCE AVAILABILITY

Lead contact

Further information and requests for resources and reagents should be directed to and will be fulfilled by the lead contact, Mitsuru Matsumoto, M.D., Ph. D (mitsuru@tokushima-u.ac.jp).

Materials availability

This study did not generate new reagents. Aire-KO, Aire/diphtheria toxin receptor (DTR)-GFP-KI and Aire/GFP-KO were previously generated in the Matsumoto's laboratory. A rat anti-mouse Aire mAb (clone MM-525) was also previously produced in the Matsumoto's laboratory.

Data and code availability

This paper analyzes existing, publicly available data (NCBI accession number: GSE155331). This paper does not report original code. Any additional information required to reanalyze the data reported in this paper is available from the lead contact upon request.

EXPERIMENTAL MODEL AND SUBJECT DETAILS

Mice

Aire-KO on B6 and BALB background (Kuroda et al., 2005) and Aire/diphtheria toxin receptor (DTR)-GFP-KI (Kawano et al., 2015) and Aire/GFP-KI (Yano et al., 2008) were reported previously. The following mouse strains were purchased from the Jackson Laboratory: CD11c-DTR/GFP-Tg. B6.FVB-*1700016L21Rik*$^{Tg\ (Itgax\text{-}DTR/EGFP)57Lan}$/J (Jung et al., 2002), Foxp3/EGFP-KI. B6.Cg-*Foxp3*^{tm2Tch}/J (Kekalainen et al., 2007), CTLA-4-KO. NOD.129(B6)-*Ctla4*^{tm1All}/DoiJ (Luhder et al., 2000) and Rag2-KO. B6(Cg)-*Rag2*$^{tm1.1Cgn}$/J. CTLA-4-KO on NOD background were backcrossed onto BALB/c or C57BL/6 background more than seven generations. C57BL/6 (B6), BALB/c (BALB) and BALB/c$^{nu/nu}$ mice were purchased from CLEA Japan. Mice aged 8–12 weeks were used for most experiments. Neonatal Aire/CTLA-4-dKO mice at the age of 9 days were analyzed (Figures 5C, S3C and S3D). Aire-KO mice at two weeks of age were used for *ex vivo* endocytosis assay (Figure S1B). All experiments were done in an age-matched manner. For thymus graft experiments, female BALB/c$^{nu/nu}$ mice at four weeks of age were used. Both male and female mice were used for all the other experiments, and there was no difference in the results between male and female mice. All mice were maintained under pathogen-free conditions and a 12-h light/12-hour dark cycle and handled in accordance with the Guidelines for Animal Experimentation of Tokushima University School of Medicine.

METHOD DETAILS

Thymic epithelial cell preparation

For thymic epithelial cells (TECs) isolation, minced thymi were digested with 0.15% Collagenase D (Roche) and 0.1% DNase I (Roche) in RPMI 1640 medium (Invitrogen) supplemented with 10% heat-inactivated FBS (Invitrogen), 2 mM L-glutamine, 100 U/mL penicillin, 100 μg/mL streptomycin, and 20mM HEPES, hereafter referred to as R10. Cell-suspensions were further digested with 0.15% Collagenase/Dispase (Roche) and 0.1% DNase I (Roche) in R10.

Flow cytometric analysis

Freshly isolated cells were used for the experiments. Information on antibodies is listed in key resources table. Following markers were used to identify the cell populations; mTECs (CD45$^-$EpCAM$^+$UEA-1$^+$), mTEC^{high} (CD45$^-$EpCAM$^+$UEA-1$^+$MHC-II^{high} or CD45$^-$EpCAM$^+$UEA-1$^+$CD80^{high}). Recombinant mouse CTLA-4 protein fused with human IgG1 (R&D Systems) (rCTLA-4/IgG fusion protein) were mixed with PE-labelled goat anti-human IgG Fcγ Ab (BioLegend) and used for the detection of CD80 and CD86 on

thymic DCs. Foxp3/Transcription Factor Staining Buffer Set (Invitrogen) was used for the staining of Aire, CTLA-4 and Foxp3. Flow-cytometric analysis was performed using a FACSAria II (BD Biosciences) as described previously (Morimoto et al., 2018). The data were analyzed using FLOWJO 10.7.1 software (TreeStar Software) or BD FACSDiva software (version 8.0) (BD Biosciences).

Single-cell (sc) RNA-seq analysis

FASTQ files were processed using Fastp, and reads were demultiplexed and mapped to the mm10 reference genome via Cell Ranger (v3.1.0). Data processing by the Cell Ranger software was performed using supercomputers HOKUSAI at RIKEN and the NIG at ROIS National Institute of Genetics. Expression count matrices were prepared by counting unique molecule identifiers. Genes that were expressed in more than 5 cells and cells expressing at least 200 genes were selected for the analysis. Seurat 3.0 (Stuart et al., 2019) and R 4.0 (https://www.R-project.org/) were used to analyze the scRNA-seq data.

In vitro endocytosis assay

To measure uptake of CD80 and CD86, recombinant CD80 (rCD80) protein and rCD86 protein fused with human IgG1 (R&D Systems) were mixed with PE-labelled goat anti-human IgG Fcγ Ab (BioLegend) at 2:1 ratio of the volume. One and half microliters of these pre-mixtures were incubated with FACS-sorted mTECs or enzymatically digested thymic cells (5×10^6 cells) from WT, Aire-KO or Aire/CTLA-4 double-knockout mice (dKO) in a total volume of 100 μL of R10 containing Fc blocker (anti-CD16/CD32 mAb; BD Biosciences) at 37°C or 4°C for three hours. Cells were then washed three times with PBS and were analyzed with a FACSAria II. Incubation with PE-labelled goat anti-human IgG Fcγ Ab without rCD80 or rCD86 served as negative controls. In some cases, rCTLA-4/IgG fusion protein (R&D Systems) was added for the inhibition. Alternatively, anti-CTLA-4 mAb labelled with allophycocyanin (APC) (clone UC10-4F10-11; BD Biosciences) was incubated with enzymatically digested thymic cells at 37°C or 4°C for three hours.

Ex vivo endocytosis assay

Thymic lobes were harvested from WT or Aire-KO at two weeks of age. Pre-mixture of rCD80 and PE-labelled goat anti-human IgG Fcγ Ab together with PE-Cy7-labelled EpCAM mAb were injected into the isolated thymi in a total volume of 15 μL per half lobe using 30G needle. Thymic lobes were then cultured on top of Nuclepore filters (Whatman) placed on R10 for four hours. TECs were harvested via enzymatic digestion as described above, and stained with anti-CD45 mAb, anti-Ly-51 mAb, anti-I-A/I-E mAb and UEA-1. Cells were analyzed for the expression of PE signals after gating for $CD45^-EpCAM^+Ly\text{-}51^-UEA\text{-}1^+MHC\text{-}II^{high}$ mTECs. Injection of PE-labelled goat anti-human IgG Fcγ Ab alone without rCD80 served as negative controls.

Immunohistochemistry

Thymi from Aire/GFP-KI (Yano et al., 2008) were fixed with 4% paraformaldehyde in PBS, and immersed in a graded series of sucrose solutions (10%, 20% and 30%). Tissues were then embedded in OCT compound (Sakura Finetek), frozen at −80°C and sectioned into 6 μm-thick slices. Samples were blocked with 2% bovine serum albumin in PBS for 1 hour and stained with anti-CD11c mAb labelled with Alexa Fluor 647 (Biolegend) and anti-GFP Ab labelled with Alexa Fluor 488 (Invitrogen) for 30 min at room temperature. Fluorescent images were visualized using All-in-One Fluorescence Microscope BZ-X810 (Keyence, Osaka) and fluorescent intensity was analyzed using a BZ-X810 analyzer software (Keyence, Osaka).

Immunocytochemical analysis

For the immunocytochemical analysis, enzymatically digested thymic cells were incubated with rCD80 protein pre-mixed with Alexa Fluor 488-labelled goat anti-human IgG (Invitrogen) at 37°C for three hours. Cells were then stained with anti-CD45 mAb, anti-EpCAM mAb, UEA-1 and anti-I-A/I-E mAb, and $CD45^-EpCAM^+UEA\text{-}1^+MHC\text{-}II^{high}$ positive for Alexa Fluor 488 cells were sorted with FACSAria II. Sorted cells were attached to the slide glass, dried at room temperature and fixed with 4% PFA. Cells were co-stained with Alexa Fluor 594-labelled anti-Lamp1 mAb (BioLegend) and DAPI (Invitrogen). Fluorescent images were visualized using All-in-One Fluorescence Microscope BZ-X810 (Keyence, Osaka) and fluorescent intensity was analyzed using a BZ-X810 analyzer software (Keyence, Osaka). To obtain high-resolution images without the blurring caused by out-of-focus fluorescent signals, optical sectioning was employed.

Reaggregate thymic organ culture

Reaggregate thymic organ culture (RTOC) was performed as previously described (Morimoto et al., 2018). Briefly, thymic lobes from E15.5 to E16.5 fetuses from WT or Aire-KO were cultured on nucleopore filter (Whatman) placed in R10 containing 1.35mM 2-deoxyguanosine (2-DG) (Sigma) for 6 days. Thymic stromal cells were prepared by dissociating thymus lobes in 0.25% trypsin (Sigma-Aldrich) and 0.02% EDTA (Wako Pure Chemical, Osaka) in PBS. Embryonic TECs (1×10^6 cells) and FACS-sorted $PI^-CD4^+CD8^-CD62L^{low}CD25^-GFP^-$ thymocytes from Foxp3/EGFP-KI (1×10^5 cells) in the presence or absence of FACS-sorted BM-APCs (2×10^4 cells) were mixed together and lightly centrifuged. Small pieces of the aggregates were taken up in a total volume of 1.5–1.8 μL by plastic tips and cultured on the surface of a nucleopore filter (Merck Millipore) placed in R10. Generation of $CD25^+Foxp3\,(GFP)^+$ mature Tregs was evaluated after digesting the reaggregates with Collagenase D (Roche) and Collagenase/Dispase (Roche) after 5 days of RTOCs.

Bone marrow transfer

Bone marrow (BM) transfer was performed as previously described (Mouri et al., 2017). In brief, BM cells were harvested from mouse femurs. Following RBC lysis, BM cells were depleted of T cells and B cells with biotinylated mAbs to CD4, CD8, CD19 (BioLegend) and Streptavidin Particles Plus-DM (BD Biosciences) according to the manufacturer's instruction. Recipient mice were irradiated with two split doses of 4.0 Gy and 3.0 Gy and were reconstituted with 1×10^7 BM cells. The mice were analyzed 2 months after BM transfer.

In vivo mouse treatment

BM chimeras receiving BM cells from CD11c-DTR/EGFP-Tg were injected *i.p.* with 600 ng of diphtheria toxin (DT) (Sigma-Aldrich) for four days, and mice were analyzed on the following day. C57BL/6 wild-type mice and BM chimeras were injected *i.p.* with 25mg/kg of either CTLA-4 Ig (ORENCIA: Ono Pharmaceutical, Osaka) or control Ig (Venoglobulin IH5%: Japan Blood Products Organization, Tokyo) at day 0, 3 and 5, and mice were analyzed four days later. For CTLA-4 blocking experiment, CTLA-4 expression/function was blocked by *i.v.* injection with 1.5mg of UC10-4F10-11 mAb (BioXCell) (Marangoni et al., 2021). Injection of Armenian hamster IgG (BioXCell) served as control. Expression of CD86 and rCTLA-4 binding for thymic and splenic BM-APCs were determined forty-eight hours after the injection.

Real-time PCR

Total RNA was extracted from TECs, Tregs and Tconvs using the RNeasy Mini Kit (QIAGEN) and converted to cDNA using the Sensiscript Reverse Transcription (QIAGEN) in accordance with the manufacturers' instructions. Real-time PCR was performed using Quantitect Probe PCR kit (QIAGEN) on Thermal Cycler Dice Real Time System II (TAKARA). The sequence of primers and probes used are listed in Table S2. For miRNA detection, total RNA was extracted from TECs using the mirVana™ miRNA Isolation Kit (ThermoFisher). Expression levels of miRNA-155 was measured using mmu-miR-155* (Assay ID: 464539_mat) from TaqMan MicroRNA Assays (ThermoFisher) on Thermal Cycler Dice Real Time System II (TAKARA).

Thymus graft

Thymus grafting onto BALB/$c^{nu/nu}$ mice (CLEA Japan) was performed as previously described (Mouri et al., 2017). In brief, thymic lobes were isolated from embryos at 15.5-day postcoitus from WT, Aire-KO or Aire/CTLA-4-dKO. The lobes were then cultured for 5 days on Nucleopore filters (Whatman) placed on R10 media containing 1.35 mM 2-deoxyguanosine (Sigma-Aldrich) to eliminate BM-derived cells within the thymus prior to the graft. Thymic lobes were then washed in fresh R10 media and transplanted under the kidney capsule of BALB/$c^{nu/nu}$ mice at 4 weeks of age. The recipient mice were used for analyses 8 weeks after thymus grafting.

Pathology

Formalin-fixed tissue sections were subjected to H&E staining, and two pathologists independently evaluated the histology without being informed of the detailed condition of the individual mouse. Histological changes were scored as none (score 0), mild (score 1), moderate (score 2) and severe (score 3).

Detection of autoantibodies

Stomach from Rag2-KO mice were harvested, embedded in OCT compound (Sakura Finetek, Tokyo), frozen at −80°C and sectioned into 6-μm-thick slices. Slices were fixed with acetone for 5 min and washed with PBS. Samples were blocked with 2% BSA in PBS for 1 hour and incubated with sera (1:300 diluted) for 1 hour at room temperature. The slides were subsequently incubated with anti-mouse IgG-Alexa Fluor 594 (Invitrogen) (1:400 diluted) for 30 min at room temperature. Reactivities were graded as none (score 0), moderate (score 1) and strong (score 2).

QUANTIFICATION AND STATISTICAL ANALYSIS

Statistical significance for the comparison of two groups was analyzed with an unpaired, two-tailed Student's t-test. One-way analysis of variance (ANOVA) coupled with Tukey's multiple comparison test was employed for the comparison of more than three groups. p values were computed using Dunn's Kruskal-Wallis Multiple Comparisons tests in GraphPad Prism for the comparison of non-parametric pathological scores from three groups. Differences were considered significant at $p < 0.05$. All the statistical details of the experiments were described in the figure legends.